Electron-Lattice Dynamics
in π-Conjugated Systems

Magnus Hultell

Department of Physics, Chemistry and Biology
Linköping University, SE-581 83 Linköping, Sweden

Linköping 2008

Author:
    Magnus Hultell
    Department of Physics, Chemistry and Biology
    Linköping University, SE-581 83 Linköping, Sweden

to my wife and our son

Abstract

The work presented in this thesis concerns the dynamics in π-conjugated hydrocarbon systems. Due to the molecular bonding structure of these systems there exists a coupling between the electronic system and the phonon modes of the lattice. If this interaction is sufficiently strong it may cause externally introduced charge carriers to self-localize in a polarization cloud of lattice distortions. These particle-like entities are, if singly charged, termed polarons. The localization length of these charged entities depends, aside from the electron-phonon coupling strength, also on the structural and energetic disorder of the system. In strongly disordered systems all electronic states become localized and transport is facilitated by nonadiabatic hopping of charge carriers from one localized state to the next, whereas in well-ordered systems, where extended states are formed, adiabatic transport models apply.

Despite great academic efforts a unified model for charge transport in π-conjugated systems is still lacking and further investigations are necessary to uncover the basic physics at hand in these systems. The call for such efforts has been the main guideline for the work presented in this thesis and is related to the topics of papers I-IV. In order to capture the coupled electron-lattice dynamics, we use a methodological approach where the time-dependence of the electronic degrees of freedom is obtained from the solutions to the time-dependent Schrödinger equation and the ionic motion in the evolving charge density distribution is determined by simultaneously solving the lattice equation of motion within the potential field of the ions. The Hamiltonian used to describe the system is derived from the Su–Schrieffer–Heeger (SSH) model extended to three-dimensional systems.

In papers I-III we explore the impact of phenylene ring torsion on delocalization and transport properties in poly(*para*-phenylene vinylene) (PPV). The physics that we are particularly interested in relates to the reduced electron transfer integral strength across the interconnecting bonds between the phenylene rings and the vinylene segments that follows from out-of-plane (phenylene) ring torsion. In papers IV and V we focus on the dynamics of molecular crystals using a stack

of pentacene molecules in the single crystal configuration as a model system, but study, in paper IV, the transport as a function of the intermolecular interaction strength, J. We observe a smooth transition from nonadiabatic hopping to an adiabatic polaron drift process over the regime $20 < J < 120$ meV. For intermolecular interaction strengths above $J \sim 120$ meV the polaron is no longer stable and transport becomes band-like. In paper V, finally, we study the internal conversion processes in these systems, which is the dominant relaxation channel from higher lying states. This process involves the transfer of energy from the electronic system to the lattice. Our results show that this process is strongly nonadiabatic and that the relaxation time associated with large energy excitations is limited by transitions made between states of different bands.

Populärvetenskaplig sammanfattning

I dagens samhälle är elektroniken ett allt viktigare och större inslag i vår vardag. Vi ser på TV, talar i mobiltelefoner, och arbetar på datorer. I hjärtat av denna teknologi finner vi diskreta komponenter och integrerade kretsar utformade främst för att styra strömmen av elektroner genom halvledande material. Traditionellt sett har kisel eller olika former av legeringar använts som det aktiva materialet i dessa komponenter och kretsar. Under de senaste 20 åren har dock såväl transistorer som solceller och lysdioder realiserats där det aktiva materialet är organiskt, d.v.s., kolbaserat.

Vi befinner oss för tillfället mitt uppe i det kommersiella genombrottet för organisk elektronik. Redan idag säljs många MP3-spelare och mobiltelefoner med små skärmar där varje pixelelementen utgörs av organiska ljusemitterande dioder (OLEDs). Denna teknologi håller nu på att introduceras i mer storskaliga produkter som datorskärmar och TV-apparater som därigenom kommer kunna göras energieffektivare, tunnare, flexiblare och på sikt också billigare. Andra tekniska tillämpningsområden för organisk elektronik som förutspås en lysande framtid är RFID-märkning, organiska solceller, och elektronik tryckt på papper, men även smarta textiler och bioelektronik har stor utvecklingspotential.

Den kanske största utmaningen kvarstår dock, att skapa elektroniska kretsar och komponenter uppbyggda kring enskilda molekyler, s.k. molekylär elektronik. Mycket snart närmar vi oss den fysikaliska gränsen för hur små komponenter som vi kan realisera med traditionella icke-organiska material som kisel. En stor drivkraft bakom forskningen på halvledande organiska material har därför varit just visionen om molekylär elektronik som inte är mer än några hundratusendelars millimeter stora. För detta ändamål krävs en mycket noggrann kontroll av tillverkningsprocesserna liksom en detaljförståelse för hur molekylerna leder ström och hur denna förmåga kan manipuleras för att realisera såväl traditionella som nya komponenter.

I denna avhandling presenteras en översikt av den fysik som möjliggör ledningsförmåga hos särskilda klasser av organiska material, s.k. π-konjugerade system, samt de forskningsresultat som utgör mitt och min handledare Prof. Sven

Stafströms gemensamma bidrag till denna disciplin. En av utmaningarna på området är den komplexitet som de organiska materialen erbjuder; laddningsprocesserna påverkas nämligen av en rad olika faktorer såsom laddningstäthet, temperatur, pålagd spänning, samt molekylernas former och inbördes struktur. I vårt arbete har vi utifrån en vidareutveckling av existerande modeller genom numeriska datasimuleringar undersökt effekten av de senare tre faktorerna på elektronstrukturen, laddnigstransporten och energidissipation i denna klass av material.

Preface

This thesis is a compilation of the work that I have carried out in the Computational Physics group at the Department of Physics, Chemistry and Biology at Linköping University in-between the fall of 2003 and the fall of 2008. It consists of two parts, where the first part aims to provide the theoretical foundation for the scientific papers presented in the second part, having in mind a reader with a general knowledge of theoretical physics.

Magnus Hultell
Norrköping, October 2008

Contents

Introduction and outline of thesis

The research presented in this thesis aims to provide a deeper insight into the dynamics of π-conjugated materials and the interplay between the electronic system and the motions of the nuclei configuration (i.e., the dynamics/vibrations of the lattice). In this chapter the aspects and applications that have guided the academic interest in the field of organic electronics over the last forty years are briefly reviewed, followed by an outline of the thesis.

1.1 A brief introduction to organic electronics

In 1967 a visiting scientist at Tokyo Institute of Technology was attempting to synthesize polyacetylene, an organic π-conjugated polymer compound, when by a fortuitous mistake a silvery thin film was formed instead of the usual black powder.[1,2] His coworker at the time, Hideki Shirakawa, later clarified the mistake as the result of having added the catalyst substance for polymerization with more than a thousand times higher concentration than intended.[3] Teaming up with researchers Alan G. MacDiarmid and Alan J. Heeger in 1976, Shirakawa made yet another surreptitious discovery. When trying to produce thin films of graphite by treating a polyacetylene film with chlorine and bromine a stepwise increase in conductivity was noticed. As it turned out, exposure to halogens increased the films conductivity by a factor of 10^7 to a level comparable to that of copper.[4,5]

The possibility for materials exhibiting the electrical properties of metals while retaining the mechanical and processing advantages of polymers was soon recognized by the research community at large. Initial interest mainly concerned the development of organic metals for use as electrical conductors, but due to poor environmental stability of the relevant materials this type of applications were never commercialized. The focus instead shifted towards the semiconducting properties

of π-conjugated materials, and in the mid 1990s a number of fundamental device applications had been realized such as organic light-emitting diodes (OLEDs),[6,7] field-effect transistors (OFETs),[8,9,10] and photovoltaic cells (OPVCs).[11,12]

Today, more than a decade later, organic electronics is at the verge of its commercial breakthrough. Light-emitting diode (LED) displays incorporating organic materials are already commercially available for portable system applications (e.g., cell phones) and television screens,[13] and the integration of polymer heterostructures is offering great hope for high-efficiency, low price organic photovoltaic cells (OPVCs).[14] Other areas where organic materials may be used for electronic applications are, e.g., smart textiles[15] and printed electronics.[16,17] In the later case, the solubility of organic materials is exploited to produce electrically functional electronic inks that can be deposited on flexible substrates such as paper or plastic films. Since all-in-line printing processes can produce printed media at a rate exceeding 100 m/min,[18] this technology may result in dramatically reduced manufacturing cost for electronics and present great opportunities for large-scale production of, e.g., radio frequency identification (RFID) tags.[18]

Despite the many promising features and applications of organic conjugated materials, and the progress made in overall performance, the field still has much room for developments. In particular, while it is generally agreed that electronic and crystal structures are related to transport characteristics, and therefore device performance, it is unclear how and to what extent.[19] In addition, algorithms that allows accurate prediction of such properties *a priori* do not currently exist. With stronger predictive capabilities, the field may develop from design based on general principles to the truly rational design of optimized materials.

To expand the knowledge on processes and phenomena that influence properties of organic materials, we present in this thesis a methodological approach to study the dynamics of organic materials at the atomistic level. This enables us to probe, e.g., transitions between adiabatic and nonadiabatic transport, and to study the dynamic properties of both conjugated polymers and molecular crystals.

1.2   Outline of thesis

The first part of this thesis, which serves as an introduction to the papers included in the second part, is organized as follows. In Chap. 2 we provide a brief account of the physical concepts and processes in π-conjugated systems relevant to the research material presented in this thesis. The information conveyed is intended for readers not previously familiar with the field and advanced readers are therefore recommended to go directly to Chap. 3 in which we focus solely on electron transfer and the different types of electron transport processes encountered in organic solids. The first two sections in particular, i.e., Secs. 3.1-3.2, provide a theoretical basis for the model Hamiltonian derived in Chap. 4, where also our methodological approach for studying electron-lattice dynamics is presented. In Chap. 5 is then provided a brief introduction to the particular research topics covered in this thesis supplemented with comments on each paper. Finally, an outlook on issues for further developments is given in Chap. 6.

Properties of π-conjugated systems

The purpose of this chapter is to give a brief overview of the fundamental processes in π-conjugated systems which are the materials of relevance in this thesis. General physical concepts related to the π-conjugated systems are presented in Secs. 2.1–2.3. In Secs. 2.4–2.5 and 2.6 charge carrier transport and electronic excitations are reviewed, respectively. For a reader already familiar with these topics it is recommended to proceed directly to Chap. 3.

2.1 Fundamental aspects

From a fundamental point of view, quantum mechanics has to be employed in order to capture the physics of a system of particles at the atomistic level. In the wave mechanical formalism of this approach the system is fully described – in the instantaneous picture – by the time-independent Schrödinger equation,

$$\hat{H}\Psi = E\Psi, \tag{2.1}$$

which is an eigenvalue equation where the eigenvalue, E, is the total energy of the system and the eigenstate, Ψ, is a mathematical wave function that describes the properties of the system, and $\hat{H}$ is the total energy operator, i.e., the Hamiltonian. This equation can be solved exactly only for a very limited number of systems containing no more than three particles. Approximations must therefore be made to both the Hamiltonian and/or to the wave function in order for larger systems to be treated quantum mechanically. A particularly useful one when illuminating the fundamental properties of the systems of interest here is the orbital approximation. At the heart of this approximation is the neglect of explicit electron-electron interaction (i.e., repulsion) which makes it possible to separate out, in turn, the coordinates of each electron and find a solution of the modified equation that is a

product of single electron wave functions. This allows us to discuss electrons as if they could be assigned and described in a system by a single orbital.

In the Born interpretation of quantum mechanics,[20,21] the wave function is considered to be a statistical quantity that only applies to an ensemble of similarly prepared systems. When discussing the position of the electron it is hence customary to discuss this in terms of spatial (orbital) regions where the probability of finding the electron in a particular state is reasonably high. In the case of atoms, the first four atomic orbitals (AOs) are labeled s, p, d, and f, which originates from a now discredited system of categorizing spectral lines as $s$harp, $p$rincipal, $d$iffuse, and $f$undamental, based on their fine structure. Alphabetical order is used beyond f.

2.2   Molecules and π-conjugated systems

When two atoms are brought together, the interactions between the constituent particles serve to modify the shape of the electron probability density regions in the isolated atoms and the atomic orbitals then no longer adequately describe the system. A new set of functions is therefore necessary to describe the diatomic molecule. These are referred to as molecular orbitals (MOs) and can be constructed, in accordance with the principle of linear superposition, from a linear combination of atomic orbitals (the LCAO MO method).[22,23] Compared to the isolated atom, the diatomic system has also undergone a splitting of the energy levels. These states can be either bonding or anti-bonding, where the later are localized outside the region of (the) two distinct nuclei and hence serves to destabilize the molecule as a whole.[a] These principles as well as the terminology adapted can be applied also to molecular systems of many atoms, where the molecular orbitals and the their spatial extension across the system are determined by the nature of the constituent elements and bonds.

In the case of the conjugated hydrocarbon systems of relevance for this thesis, three of the four atomic orbitals of carbon associated with the valence electrons of the outermost occupied shell overlap topside-on along the internuclear axises to form covalent σ-bonds. A σ-bond has cylindrical symmetry around the internuclear axis (see Fig. 2.1(a)), and is so called, because when viewed along the internuclear axis it resembles a pair of electrons in an s orbital (and σ is the Greek equivalent of s). The remaining $2p_z$-atomic orbitals are directed perpendicular to the σ-bond plane and overlap broadside-on to form a π-bond, so called since, when viewed along the internuclear axis, they resemble a pair of electrons in a p orbital (and π is the Greek equivalent of p), as seen in Fig. 2.1(b). This overlap is much weaker than that of topside-on overlap, and as a consequence thereof the energy level splitting for π-electron states will be considerably smaller than for the σ-electron states. This is important since the energy gap of the former is large compared to observed energies for, e.g., phonons and charge carriers within these systems. The physics of these species must therefor depend primarily on the π-electrons of the electronic system.

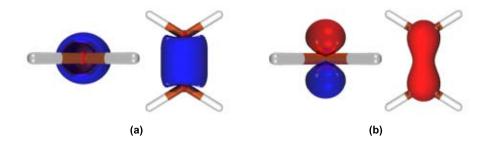[a]Note that anti-bonding MOs are usually higher in energy than bonding MOs.

(a) **(b)**

Figure 2.1. The molecular orbitals associated with (a) the σ-bond and (b) the π-bond (b) in ethylene ($H_2C{=}CH_2$) between the two sp^3-hybridized carbon atoms, viewed both along and perpendicular to the internuclear axis.

By analyzing the overlap between π-orbitals (see for example Sec. 4.2) it is found that there exists a coupling between the π-electrons and nuclei distortions, commonly referred to as the electron-phonon (e-ph) coupling. This has important implications for the properties of the system. First of all, the e-ph coupling is responsible for the particle-like entities formed when introducing extra charges into a charge neutral system. The first charge that enters the system will polarize its surrounding and effectively self-trap in the potential of the lattice distortions (phonons) to form a localized state referred to as a polaron. If the charge under consideration is taken to be an electron it will, upon entering an unoccupied anti-bonding state, serve to stabilize this state while destabilizing the associated occupied bonding state. Introducing the concept of an energy gap as the forbidden region of energies in between the highest occupied molecular orbital (HOMO) level and the lowest unoccupied molecular orbital (LUMO) level, polaron formation is found to cause these levels to migrate into this energy gap. This stabilization-destabilization effect is even further promoted if a second electron is allowed to enter the unpaired anti-bonding state, the corresponding particle-like entity of which is referred to as a bipolaron. Additional electrons introduced into the system will serve to increase the density of polaronic and bipolaronic states within the original band gap. Another implication of the large energy gap associated with σ-electrons is that they are strongly localized to the covalent bonds in which they participate. In more formal treatments of π-conjugated systems it is therefore customary to invoke σ-π separability, i.e., to treat the contributions from the σ- and π-electron subsystems separately.

2.3 Semiconducting organic solids

Even though electronics at the molecular level have been devoted considerable academic interest ever since the suggestion of a molecular rectifier by Aviram and Ratner,[24] most practical applications are today concerned with the properties of systems consisting of a very large number of molecules. With reference to the previous discussion, we shall refer to the mathematical functions describing the states of electrons within these systems as molecular crystal orbitals (MCOs) even

though these materials seldom display structural crystallinity. Introducing the concept of a density of states (DOS) as the number of states at each energy level that can be occupied by an electron, the density of occupied states (DOOS) per unit volume at a given energy[b] can then be obtained as the product of the DOS and the probability distribution for the likelihood that a particular state will be occupied by an electron (as given by Fermi-Dirac statistics). Studying the DOOS of well-ordered structures it is found that the differences between the energy levels of the MCOs are small, so that the levels may be considered to form "continuous" bands of energy rather than the discrete energy levels of the molecules in isolation. These regimes of very high density of states are separated by intervals where no energy levels except those of impurities and structural defects are found. We shall refer to these intervals as energy gaps.

At absolute zero, the probability of occupation provided from Fermi-Dirac (FD) statistics is given by a step function where occupation is allowed only below a certain energy referred to as the Fermi level. For the intrinsic system this means that states in energy bands that lay below this level will be completely occupied, whereas states in the bands that lay above this level will be completely empty. Using terminology adapted from solid state theory, the two bands immediately above and below this level will be referred to as the conduction band and the valence band, respectively. At nonzero temperatures the FD probability function "smooths out" and as a consequence thereof an appreciable number of states both above (below) the Fermi level will be filled (empty).

The density of states in the valence and conduction bands can be directly related to the chemical structure of the material. If the system is highly ordered, as in molecular single crystals, there is a narrow spread in energy and the density of state is large. Positional disorder in these systems serves to broaden the DOS as it becomes increasingly difficult for electrons to acquire the energy necessary to populate energetically and spatially available MOs and the spatial region to which the electron is localized thus shrink. The opposite is of course also true and is often related to favorable molecular packaging.[25] From a physical point of view this can be understood on the basis of the increased topside-on overlap between π-orbitals on different molecules as these are stacked in increasingly parallel configurations. In the well-ordered molecular single crystals the overlap can be both strong and uniform and the localization length therefore long, whereas in disordered organic solids for which the intermolecular overlap is weak, the electrons will become strongly localized.

2.4   Charge transport in organic semiconductors

In strongly disordered system all states are localized and the DOS is assumed to have a broad Gaussian shape[26] (as schematically illustrated in Fig. 2.2(a)). The elementary transport event in such systems is then the transfer of a charge carrier between adjacent transporting molecules or segments of a main chain polymer, as described by hopping models when the electron-phonon (e-ph) coupling

---

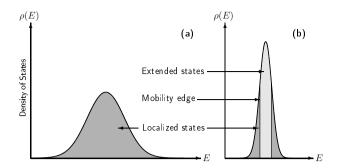[b]For the system at thermal equilibrium

Figure 2.2. The density of state (DOS) as envisioned in (a) disordered organic solids and (b) more well-ordered systems. Note that E denotes the energy of the state.

is weak and by small polaron models when the e-ph coupling is strong. In both models electron transfer is assumed to be promoted by absorption and emission of phonons. The transition rate equations in the case of the former is well approximated by the rate equations obtained by Miller and Abraham[27] for electron transfer in amorphous semiconductors, and in the case of small polaron hopping by Marcus theory[28] and/or the Holstein-Emin model.[29,30]

With increasing order, delocalized states will be able to form. A mobility edge energy may therefore be envisioned,[31,32] presumably sharp at low temperatures,[33] that separates localized states from delocalized states. The tail sites of the Gaussian DOS assumed for the highest occupied and lowest unoccupied band of MCO states of the system therefore act as continuous pseudo-exponential traps[34] to the transport band of the delocalized states (as illustrated in Fig. 2.2(b)). Further discrete trapping levels exist in the carrier energy gap due to chemical impurities and molecular defects. In these systems two transport mechanisms exists in parallel: (i) adiabatic transport through delocalized states limited by phonon scattering and (ii) thermal release of electrons trapped in localized states (as described by, e.g., the multiple trap and release (MTR) model). The later is dominant at low temperatures, where thermal activations transfer the carriers from the distribution of trapping centers to the transport band, where they diffuse for a while until they are trapped again. As the temperature of the system increases, the time spent in trapped states will start to decrease and eventually the scattering of electrons due to phonons will become the rate limiting process for charge transport. For ultrapure oligoacene single crystals, Karl[35] has shown that the scattering regime can be extended to very low temperatures where, in principle, band theory could be used as a model for charge transport.

With reference to this discussion we present in Fig. 2.3 a taxonomy of transport models for intrinsic systems organized with respect to the relative dependence of (i) the electron-phonon (e-ph) coupling strength, which determines the extent of the charge carriers polaronic signature, and (ii) the disorder in the system as primarily introduced via conformational distortions and chemical defects, commonly referred to as structural and energetic disorder, respectively. These models will be discussed in further detail in Chap. 3, organized with respect to the (dis)order of the systems
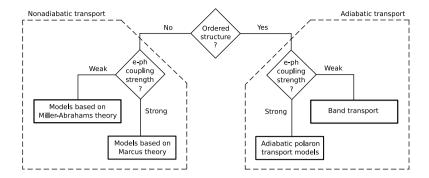
Figure 2.3. Flow chart taxonomy of transport models in semiconducting organic solids.

to which the models apply. Note that the discussion will also encompass the MTR model, excluded from the taxonomy since it accurately describes transport only at very low temperatures in well-ordered systems. Finally, it should be emphasized that the taxonomy presented in Fig. 2.3 is not intended to be exhaustive, but rather to provide a framework to be used as a reference when discussing models that aims to describe transport in the intermediate regimes.

2.5 Characterization of charge transport

The key quantity that characterizes a materials ability to transport charge is the mobility, μ. For electric field-induced (drift) charge transport, which dominates the migration of charges across an organic layer in a device, μ is defined as the ratio between the field-induced directional velocity component of the mobile charge carriers,[c] $\langle v \rangle$, and the applied electric field, E; that is:

$$\mu = \langle v \rangle / E, \tag{2.2}$$

where From our previous discussion we expect charge carrier mobilities to be influenced by molecular packaging, disorder, presence of impurities, and temperature (T), but also other factors need to be considered such as the electric field strength (since $\langle v \rangle = \mu \cdot E$ is usually linear for not to high fields[35]) and the charge carrier density, n.[36]

To illustrate the complexity of these dependencies we present in Fig. 2.4 a cartoon adapted from the measurements of Podzorov *et al.*[37] on the temperature dependence of mobility along two crystallographic axes in a rubrene single crystal. This is a very well-ordered system, and we interpret the knee in the $\mu(T)$-dependence as the transition from a trapping and releasing temperature activated regime to a temperature deactivated regime due to scattering. We also observe an evolving anisotropic behavior in $\mu(T)$ during the transition between the two charge carrier mechanisms. The reason for this is the lower than cubic symmetry of

---

[c]Note that this specification implies a drift motion superimposed on their thermal motion as a time and ensemble average of a fast sequence of acceleration and scattering events.
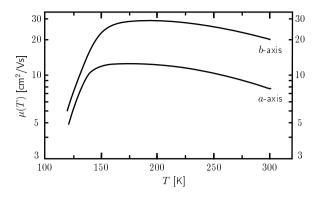
Figure 2.4. The mobility (μ) as a function of temperature (T) upon cooling a well-ordered molecular crystal.

molecular crystals that results in more extended states along some crystallographic directions compared to others and that this property reveals itself first when the motion of charge is dominated by drift rather than trapping and releasing.

In practice, charge transport measurements are influenced by a variety of extrinsic parameters, such as air exposure, humidity, device geometry, charge carrier injection. Therefore, first of all, reliable experimental data are required to find out how large the intrinsic transport parameters are and under which conditions which kind of transport model can be applied.

2.6 Excitation and relaxation dynamics

In organic photovoltaic (OPV) components such as organic solar cells (OSCs) and organic light emitting diodes (OLEDs), the fundamental physics concerns the absorption or emission of light in the active organic material. At the microscopic level, these processes involve electronic transitions to higher (excitation) or lower (emission) energy states by the absorption or emission of photons.

The work in Paper V is related to the relaxation process following an excitation of an electron to an anti-bonding state above the band gap. In what follows we shall briefly outline the photophysics of electronic transitions with respect to electron-phonon dynamics. References are made to the schematic drawing in Fig. 2.5 of the (a) classical and (b) quantum mechanical picture of an electronic transition between the ground state Ψ^{gs} and the excited state Ψ^{es}. Note that the potential energy of each electronic state is expressed in terms of the normal coordinate (q) of the system.

The system is initially in its ground state configuration (q^{gs}). Upon absorption of a photon from the incident light, an electronic transition is made from a bonding to an anti-bonding state. Since this transition is much faster than the response time of the nuclei, the molecular geometry will remain unchanged immediately after the excitation. However, during the transition, the electron density is rapidly built up in new regions of the nuclei and removed from others, and the nucleus suddenly
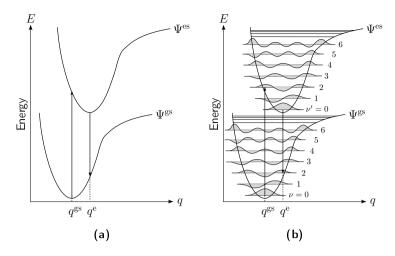
Figure 2.5. Illustration of the (a) classical and (b) quantum mechanical picture of an electronic transition. In (b) the transition between $\nu = 0$ and $\nu' = 2$ is favored.

experiences a new force field, i.e., a new potential (upper curve). The response of the nuclei is that they start to vibrate. Relaxation may now proceed due to either (i) radiative emission of a photon, (ii) vibrational cooling of the same electronic state, or (iii) phonon-assisted transitions between two different electronic states. The later process, termed internal conversion (IC), is usually the fastest relaxation channel and provides efficient sub-picosecond nonradiative transfer from higher to lower excited states.[38] As a result the vast majority of (organic) molecular systems follow Vavilov-Kasha's rule, stating that radiative emission typically occurs from the lowest excited electronic state.[39] The fact that $q^e > q^{gs}$ for this state, where q^e is the energetically most favorable configuration of the excited system, follows from the anti-bonding character of the excited state molecular orbital which gives rise to an elongation of one or several bonds in the molecules.

There are aspects of the excited state dynamics that due to methodological reasons never enter the numerical simulations which we use to explore the physics of certain relaxation processes. Some of these at least are important for the operation of real devices and a brief discussion is therefore in order. When an electron makes a transition to an excited state it leaves behind a hole of positive charge to which it is bound by Coulomb interactions. The bound electron-hole pair is commonly referred to as an exciton. Exciton dynamics is vital for both organic solar cells and light emitting diodes. In case of the former, excitons are formed when the material absorbs energy from the incident light. To be able to harvest this energy in the form of a photocurrent it is vital that these excitons do not recombine (radiative emission of a phonon) before they encounter a quenching site where they can dissociate into free carriers and be collected by the electric field applied across the device. In a light emitting diode, where radiative recombination is desired, the problem is reverted to getting the electrons and holes injected into the material to form excitons.

Electron transfer

The focus of this chapter is to provide a detailed picture of charge carrier transport processes in π-conjugated systems. In particular, we consider a situation when an excess electron has been injected into the system and present in Secs. 3.1-3.2 an archetypal model Hamiltonian for intersite electron transfer processes. The main purpose of this effort is to provide a theoretical background for the Hamiltonian which we employ in our own studies of the coupled electron-nuclei dynamics, the methodological approach of which is developed in Chap. 4. Other issues that are reviewed in this chapter centers around the influence of the strength of the electron-phonon coupling constant and the impact of both energetic and structural disorder on the transport properties of π-conjugated systems of many molecules, as presented in Secs. 3.3-3.6.

3.1 The electron transfer Hamiltonian

In the following two sections a Hamiltonian for the transfer of excess electrons is derived. In this description we introduce an effective potential experienced by the excess electron after entering the system:

$$V(\mathbf{r}) = \sum_m V_m(\mathbf{r}), \tag{3.1}$$

where each contribution $V_m(\mathbf{r})$ can be understood as a so-called pseudo-potential which mimics the action of the total electronic system of molecular fragments, m, on the excess electron. Here, we define the various $V_m(\mathbf{r})$ by requiring that their ground state energy level E_m should coincide with the electronic ground

state of the isolated molecular unit plus the excess charge.[a] The pseudo-potential enters the single particle Schrödinger equation which determines the single-particle energies E_m and single-particle wave functions $|\varphi_m(\mathbf{r})\rangle$, respectively:

$$[T_{\rm el} + V_m(\mathbf{r})]|\varphi_m(\mathbf{r})\rangle = E_m|\varphi_m(\mathbf{r})\rangle. \tag{3.2}$$

Since the energies E_m corresponds to different sites in the system, they are usually called (on)site energies.

At this stage we can now write the total electronic Schrödinger equation on the following form:

$$[T_{\rm el} + V(\mathbf{r})]|\phi\rangle = \mathcal{E}|\phi\rangle. \tag{3.3}$$

Expanding the wave function in a linear combination of $|\varphi_m(\mathbf{r})\rangle \equiv |\varphi_m\rangle$, i.e.,

$$|\phi\rangle = \sum_m c_m|\varphi_m\rangle, \tag{3.4}$$

inserting Eqn. (3.4) into Eqn. (3.3), and multiplying the equation on both sides by $\langle\varphi_n|$ from the left, gives

$$\sum_m c_m \left(E_m\langle\varphi_n|\varphi_m\rangle + \sum_{k\neq m}\langle\varphi_n|V_k|\varphi_m\rangle \right) = \mathcal{E}\sum_m c_m\langle\varphi_n|\varphi_m\rangle. \tag{3.5}$$

This set of equation contains both the overlap integrals, $\langle\varphi_n|\varphi_m\rangle \equiv S_{nm}$, and the three-center integrals $\langle\varphi_n|V_k|\varphi_m\rangle$. The later are by far the most numerous to evaluate and since their contribution is small compared to the one- and two-center integrals they are often neglected by assuming zero differential overlap (ZDO) within the system (also known as the Pople approximation).[40] As suggested by its name, it also follows from this approximation that the two-center overlap integrals will be neglected, i.e., we set $S_{nm} = \delta_{nm}$.[b] In essence, this means that the states $|\varphi_m\rangle$ form an orthogonal basis. Of the surviving one- and two-center integrals the latter contain terms of either the type $\langle\varphi_m|V_k|\varphi_m\rangle$, which introduce a shift of the onsite energies E_m due to the presence of the pseudo-potential V_k at site k, or of the type $\langle\varphi_n|V_n|\varphi_m\rangle$, which couples the state $|\varphi_m\rangle$ to the state $|\varphi_n\rangle$ via the tail of the potential V_n at site m.

An expansion of the electronic part of the Hamiltonian gives that

$$H_{\rm el} = \sum_{m,n}\langle\varphi_m|H_{\rm el}|\varphi_n\rangle|\varphi_m\rangle\langle\varphi_n|, \tag{3.6}$$

with $\langle\varphi_m|H_{\rm el}|\varphi_n\rangle \equiv H_{mn}$ given by

$$H_{mm} = E_m + \sum_{k\neq m}\langle\varphi_m|V_k|\varphi_m\rangle, \tag{3.7}$$

$$H_{mn} = \langle\varphi_m|T_{\rm el} + V_m + V_n|\varphi_n\rangle. \tag{3.8}$$

---

[a]It is thus taken into account that the full many-electron wave-function adjust itself during the transfer process, although it is carried out by reducing the many-particle dynamics to the action of an effective local single-particle potential.

[b]Note that the Kronecker delta δ_{nm} is defined such that δ_{nm}=1 for m=n, and 0 otherwise.

The matrix elements $H_{mn} \equiv V_{mn}$ are commonly referred to in literature as transfer integrals or alternatively inter-state coupling elements. Including the diagonal matrix elements of the pseudo-potentials into the definition of the site energies E_m, the electronic Hamiltonian for the system reads

$$H_{\text{el}} = \sum_m E_m |\varphi_m\rangle\langle\varphi_m| + \sum_{m,n} V_{mn} |\varphi_m\rangle\langle\varphi_n|. \qquad (3.9)$$

3.2 The electronic-nuclei Hamiltonian

Adding also the nuclei degrees of freedom, $\{R_u\} \equiv R$, to the electronic Hamiltonian (see Eqn. (3.9)), the "complete" electronic-nuclei Hamiltonian becomes

$$\begin{aligned} H &= H_{\text{el}}(R) + T_{\text{nuc}} + V_{\text{nuc-nuc}}(R) \\ &= \sum_m \left[(T_{\text{nuc}} + E_m(R) + V_{\text{nuc-nuc}}(R)) + \Theta_{mm} \right] |\varphi_m\rangle\langle\varphi_m| \\ &\quad + \sum_{m \neq n} \left[V_{mn}(R) + \Theta_{mn} \right] |\varphi_m\rangle\langle\varphi_n|, \end{aligned} \qquad (3.10)$$

where T_{nuc} denotes the kinetic energy of all nuclei coupled to the electron transfer process and $V_{\text{nuc-nuc}}(R)$ results from the coupling among the vibrational degrees of freedom (i.e., electrostatic coupling among the nuclei). Note that the nonadiabaticity operators Θ_{mn} have been introduced into Eqn. (3.10) to account for the dependence of the expansion states $|\varphi_m\rangle$ on the vibrational coordinates.

In the following, we assume that the nonadiabatic coupling is small and neglect its contribution to the off-diagonal part of the Hamiltonian in Eqn. (3.10). This assumption is motivated by the localization of the wave functions $\varphi_m(\mathbf{r})$ at the various units of the system. With reference to the specific form of H we also introduce potential energy surfaces (PESs) which relate to those states with the excess electron localized at site m:

$$U_m(R) = E_m(R) + V_{\text{nuc-nuc}}(R) + \Theta_{mm}, \qquad (3.11)$$

such that the total electron-vibrational Hamiltonian is obtained as

$$H = \sum_m \left[(T_{\text{nuc}} + U_m(R)) \right] |\varphi_m\rangle\langle\varphi_m| + \sum_{m \neq n} V_{mn}(R) |\varphi_m\rangle\langle\varphi_n|. \qquad (3.12)$$

Not yet commented, we note that the inter-site couplings V_{mn} depend on the nuclear coordinates. Since the magnitude of V_{mn} is mainly determined by the overlap of the exponential tail of the wave functions localized at sites m and n, it is reasonable to expect an exponential dependence on inter-site distance, x_{mn}, of the form

$$V_{mn}(R) = V_{mn}^{(0)} \exp\left\{ -\beta_{mn}(x_{mn} - x_{mn}^{(0)}) \right\}. \qquad (3.13)$$

Here, $V_{mn}^{(0)}$ is the reference value of the inter-site couplings reached for the reference (equilibrium) distance $x_{mn}^{(0)}$ and β_{mn} is some characteristic inverse length

determined by the wave function overlap. It should be emphasized that the dependence of V_{mn} on R is often neglected in comparison with the on-site vibrational dynamics. We will use this simplification in the following section when discussing different regimes of electron transfer.

3.3 Regimes of electron transfer

Before we proceed to discuss the transport processes in organic solids it is useful to first understand the physics of the simplest electron transfer (ET) system possible, i.e., the two-state system where the transfer is from a donor state (D) to an acceptor state (A). To keep things as simple as possible, we neglect any dependence of V_{DA} on the nuclear coordinates, i.e., $V_{DA}(R) \simeq V_{DA}$. The electronic-nuclei Hamiltonian (see Eqn. (3.10)) for this two-state model then read

$$H_{DA} = H_D|\varphi_D\rangle\langle\varphi_D| + H_A|\varphi_A\rangle\langle\varphi_A| + V_{DA}|\varphi_D\rangle\langle\varphi_A| + V_{AD}|\varphi_A\rangle\langle\varphi_D|, \quad (3.14)$$

where $H_{A(D)} = T_{\text{nuc}} + U_{A(D)}(R)$. Note though that in the following paragraph we use the reduced index m for both the acceptor (A) and the donor (D).

The dependence on the nuclear coordinates can be made more concrete by introducing PESs which depend on normal mode coordinates $\{q_\xi\} \equiv q$. In this case it is advantageous to choose a particular electronic state as a reference state to define a reference configuration of the nuclei. This state is supposed to be characterized by the PES $U_m(R)$ having the equilibrium configuration at $\{R_u^{(m)}\} \equiv R^{(m)}$, where u is a site index for the nuclei. Carrying out an expansion of $U_m(R)$ around $R^{(m)}$ up to second order with respect to the deviations $\Delta R_u^{(m)} = R_u - R_u^{(m)}$ (the harmonic approximation) we obtain, after a linear transformation to (mass-weighted) normal mode coordinates, a parabolic PES $U_m(q)$ of the form:
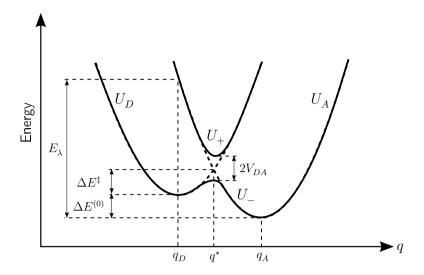
$$U_m(q) = U_m^{(0)} + \frac{1}{2}\sum_\xi \omega_{m,\xi}^2 (q_\xi - q_\xi^{(m)})^2. \quad (3.15)$$

Using this definition and the fact that the vibrational kinetic energies are not affected by this transformation, we obtain PESs for the complete system of the form

$$U_\pm(q) = \frac{1}{2}\left(U_D(q) + U_A(q) \pm \sqrt{(U_D(q) + U_A(q))^2 + 4|V_{DA}|^2}\right). \quad (3.16)$$

These adiabatic PESs, together with the diabatic PES for the donor (U_D) and the acceptor (U_A) state, are plotted in Fig. 3.1 versus a single coordinate q. We note that at the crossing point q^* of the two diabatic PES, defined by $U_D(q^*) = U_A(q^*)$, there is, according to Eqn. (3.16), a splitting between the adiabatic PES by $2|V_{DA}|$. This splitting becomes smaller if q deviates from q^* and the adiabatic and diabatic curves coincides for $|q - q^*| \gg 0$.

Which type of representation is more appropriate depends on the problem under discussion. When the inter-site coupling is *weak* both the donor state and the adiabatic state are spatially rather separated with only a small fraction of

Figure 3.1. The donor (U_D) and acceptor (U_A) potential energy surfaces (PESs) are plotted versus a single process (reaction) coordinate (q). The diabatic curves U_D and U_A are represented by dashed line, whereas the adiabatic curves U_+ and U_- are drawn with full lines. Also shown are the activation barrier energy $\Delta E^{\ddagger}$ for nonadiabatic ET, the driving force $\Delta E^{(0)} = U_D^{(0)} - U_A^{(0)}$, and the splitting between the adiabatic curves with a magnitude of $2V_{DA}$ at the crossing point q^*.

the electron probability density reaching the donor state. For this type of situations the *diabatic* (or *nonadiabatic*) representation is adequate and carrying out a perturbation expansion with respect to V_{DA}, where the diabatic states represent the zeroth-order states, it is found that the electron transfer (ET) rate becomes proportional to $|V_{DA}|^2$, but that it also depends on the probability at which the crossing region on the donor PES U_D is reached by the vibrational coordinates. Accordingly, the electron transfer rate, k_{ET}, is expected to be of the following form:

$$k_{ET} \propto |V_{DA}|^2 e^{-E_{\text{act}}/k_B T}. \tag{3.17}$$

Note that since, in the lowest order of perturbation theory, ET occur when the donor and acceptor levels are degenerate, E_{act} here denotes the activation energy needed to enter the crossing region starting at the minimum position of the donor PES, i.e., $E_{\text{act}} = U_D(q^*) - U_D(q_D)$.

Within the framework of nonadiabatic ET, an illustrative example of these dependencies is obtained in the high-temperature limit, where $k_B T \gg \hbar\omega_\xi$ for all phonon modes ξ and a description of the vibrational dynamics using classical physics therefore is valid. Assuming parabolic PESs and vibrational frequencies independent of the electronic state, it is then possible to show that (with reference to the two-level system displayed in Fig. 3.1):

$$k_{\text{ET}} = \frac{2\pi}{\hbar} \frac{1}{\sqrt{4\pi E_\lambda k_B T}} |V_{DA}|^2 \exp\left\{-\frac{(\Delta E^{(0)} + E_\lambda)^2}{4 E_\lambda k_B T}\right\}. \tag{3.18}$$

Here, E_λ is the reorganization energy, $\Delta E^{(0)} = U_D^{(0)} - U_A^{(0)}$ is the driving force, and $(\Delta E^{(0)} + E_\lambda)^2/4E_\lambda \equiv \Delta E^\ddagger$ is the activation energy for nonadiabatic ET. Equation (3.18) is usually referred to as the Marcus formula after R. A. Marcus, who pioneered the theory of ET starting in the 1950s.[28,41,42,43,44] The main advantage of this rate equation is that it describes the complex vibrational dynamics accompanying the electronic transition by a small number of parameters, namely the inter-site coupling V_{DA}, the driving force ΔE, and the reorganization energy, E_λ. It should be emphasized, though, that a more elusive model for ET is required in the low-temperature regime ($k_B T \ll \hbar\omega_\xi$), where tunneling effects become important and phonons needs to be considered quantum mechanically.

In the case when the inter-site coupling is *strong*, the electronic states are expected to extend over several sites and it becomes advantageous to change from the (nona)diabatic to the adiabatic representation. When the states extend over the full width of the system they are referred to as delocalized. The electron transfer process involves in the case of extended states a gradual shift of the electronic wave function from the donor site to the acceptor site intimately connected with the rearrangement of the vibrational degrees of freedom from q_D to q_A. This rearrangement is connected with a barrier crossing, and we expect for the ET rate an expression of the standard Arrhenius type:
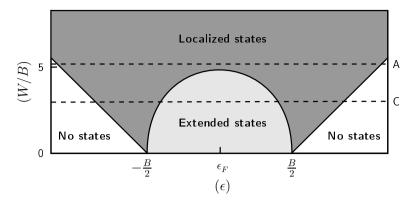
$$k_{ET} \propto e^{-E_{\text{act}}/k_B T}. \tag{3.19}$$

Note though that the activation energy E_{act} is different from the one appearing in the nonadiabatic ET rate equation (Eqn. (3.17)), and here refers to the barrier in the lower adiabatic PES U_- (Eqn. (3.16)).

3.4 The impact of disorder

When systems with *many* transport sites are considered it turns out that the transfer of electrons is strongly influenced by the distribution of values in both E_m and V_{mn}, commonly referred to in literature as diagonal- and off-diagonal disorder, respectively. An early model for diagonal disorder was introduced by P. W. Anderson[45] in which the onsite energies E_m are chosen randomly with equal probability in the range $E_m \in [-W/2, W/2]$ (box distribution). Furthermore, the energy scale is fixed by setting the hopping integrals between nearest-neighbors to unity and zero otherwise. With respect to the bandwidth, B, of the energy levels, Anderson showed that once the disorder exceeds a critical value, $(W/B)_{\text{crit}}$, the solutions of the Schrödinger equation for any energy band are no longer the extended states of Bloch, but are localized in space so that an electron can move from one site to the other only by exchanging energy with phonons.[c] It was later pointed out by Mott[46,47] that localized states will exist near the extremities of a band even if (W/B) lies below the critical value, and that an energy E_c must separate energies where states are localized from energies where the states are

---

[c]It should be pointed out that the transition between localized and extended states is only observed in three-dimensional systems and that localization occur for any non-zero disorder introduced in one- and two-dimensional systems.

Figure 3.2. Localization of states as a function of the ratio between the width of the onsite energy distribution, W, and the band width, B. Note that the cross section at A and C (dashed line) corresponds to Figs. 2.2(a) and 2.2(b), respectively.

extended. This is the mobility edge previously discussed in Sec. 2.4. A schematic illustration of the results of the analysis of Anderson and Mott are displayed in Fig. 3.2. In this context it should be noted that similar results are expected to hold also for off-diagonal disorder.

It is important to recognize that diagonal and off-diagonal disorder are directly related to the energetic and the structural disorder of the real system, where the former is due to chemical defects and impurities, and the later a consequence of conformational distortions. Synthesis and film preparation techniques are hence critical in the construction of organic electronic devices that rely on high mobilities in the active layer(s). This explains, e.g, why the highest mobilities so far observed has been measured in organic devices with ultrapure well-ordered molecular single crystals as the active layer.[35,37] It should be emphasized, though, that these materials, although very useful for obtaining basic physical insight, will have no chance in technical electronic applications because of their poor mechanical properties. Rather, organic thin films with as high structural and energetic order as possible should be considered the true candidates.[35]

In the following two sections some of the many models suggested in literature for use in analyzing transport characteristics in dis-/ordered materials will be reviewed, for which a crude and by no means exhaustive taxonomy was presented in Fig. 2.3 in Chap. 2.

3.5 Charge transport in disordered systems

In many polymer solids the molecules are subjected to considerable spatial (and often also energetic) disorder and the elementary transport event is the nonadiabatic transfer of a charge carrier between adjacent transporting molecules or segments of a main chain polymer, henceforth referred to as transport sites. For such transfer processes to occur the charge carrier needs to overcome the potential

energy barrier between the two localized states. This may be achieved either by (i) emitting or absorbing phonons, or (ii) by simply tunneling from one state to the other. The former process is thermally activated and by far the most dominant transport mechanism at room temperature in disordered organic solids. The associated activation barrier is, in general, related to both intermolecular as well as intramolecular interactions, the first of which arises from the physical nonequivalence of the hopping sites, whereas the latter is due to the change in molecular conformation upon removal/addition of an electron from/to the transport site. Transfer of charge then requires the concomitant activated transfer of the molecular distortion, i.e., transfer of a polaron. The essential difference among transport models is related to the relative importance of these two contributions. When the coupling between the charge carrier and the intra(or inter)molecular modes is weak, hopping models apply with distributions in activation energies for electron transfer that serves to reflect the disorder associated with the transport sites. The (small) polaron model, on the other hand, considers the disorder energy negligible relative to the molecular deformation energy.

Hopping in the absence of polaronic effects is usually treated in terms of Miller-Abrahams hopping,[48] which is a special case of the more general Holstein-Emin equation.[29,30] Within Miller-Abrahams formalism the hopping rate from an initial (donor) site i with energy ϵ_i to a final (acceptor) site f with energy $\epsilon_f = \epsilon_i + \Delta E$ can be expressed as[27]

$$k_{\text{ET}} \equiv \nu_{if} = \nu_0 \exp(-2\alpha R_{if}) \begin{cases} \exp(-\Delta E/k_B T), & \Delta E \geq 0, \\ 1 & \Delta E \leq 0, \end{cases} \tag{3.20}$$

where the pre-factor $\nu_0 \propto |V_{if}|^2$ is the attempt-to-jump frequency, R_{if} is the distance between the initial and final site, and α is a decay factor which takes into account the decay of the inter-site coupling with distance. Accordingly, jumps upwards in energy are thermally activated, as they involves the absorption of an available phonon, whereas jumps downwards in energy is temperature independent and involves the emission of a phonon. The actual hopping rate will be determined by the competition between the two exponential factors in Eqn. (3.20). An important observation in this context is that while at small distances the first exponential factor in Eqn. (3.20) will be large, the chance of finding sites that are close in energy is small. Hence, the rate of hopping between nearest neighbors could be smaller than that between sites farther apart but closer in energy. This type of reasoning gave rise to the so-called variable range hopping (VRH) model in which carriers jump between sites for which the range $\mathcal{R} \equiv 2\alpha R_{if} + \Delta E/k_B T$, i.e., the rate, is the highest.[49,50,51] As a final remark to the Miller-Abrahams hopping rate it should be emphasized that only single acoustic phonon transitions are accounted for and no consideration is taken to include polaronic effects. When applied to organic materials, Eqn. (3.20) should therefore merely be considered as a phenomenological expression for the hopping rate.

If the charge carriers transferred through a system acquires a polaronic character, Eqn. (3.20) no longer holds and the hopping rate is rather obtained from the Marcus or (small) polaron theory.[28,44,52,53,54] Details of the derivation from a general expression for a polaron hopping rate in disordered organic systems

to formulations for different temperature regimes have been provided by Jortner and Bixon[55,56] and Schatz and Ratner.[53] In particular, it is noted that the classical result originally derived by Marcus (see Eqn. (3.18)) is obtained from the more general expression derived by Jortner[55] in the low temperature regime. By comparing the classical Marcus rate equation with those presented by Miller and Abrahams, we note that the rate in the former will decrease if $\Delta E < -E_\lambda$, a region which is commonly referred to as the Marcus inverted region and which is completely absent in the Miller-Abrahams model. Another important observation from Eqn. (3.18) is that the rate, while increasing with increasing temperature at low temperatures, T, where the exponential factor dominates, will decrease with temperature at high T due to the $1/\sqrt{T}$ prefactor.

In disordered materials the hopping rate will vary from site to site due to variations in the onsite energies and the inter-site coupling. Consequently, for disordered systems, general analytical expressions for the mobility based on the hopping rates discussed above are difficult to obtain. Using the alternative approach of Monte Carlo simulations, Bässler demonstrated that hopping theory based on Miller-Abrahams formalism and a Gaussian distribution of onsite energies[d] (with width σ_{DOS}) could reproduce many of the observations made in experiments on, e.g., molecularly doped polymers.[48] In particular, he found that the dependence of mobility, μ, on electric field strength, E, and temperature, T, within this approach, commonly referred to as the Gaussian disorder model (GDM), can be described by:

$$\mu = \mu_0 \exp[-(2\hat{\sigma}/3)^3 + C(\hat{\sigma}^2 - \Sigma^2)\sqrt{E}], \tag{3.21}$$

where μ_0 is the mobility in the limit $T \to \infty$ and $E \to 0$, C is a constant determined from simulations, $\hat{\sigma} = \sigma_{\mathrm{DOS}}/k_B T$ is the width of the DOS relative to $k_B T$, and Σ describes the off-diagonal disorder. Since Eqn. (3.21) has been widely used to analyze experiments under the assumption that μ_0, σ_{DOS}, and Σ completely characterize any given material, with σ_{DOS} representing the width of the DOS due to all sources of energetic disorder, a few remarks are in order. (i) From experiments it is well known that the dependence of mobility on the strength of the electric field follows a characteristic Poole-Frenkel (PF) like $\mu \propto \exp(\gamma\sqrt{E})$ behavior, with γ being a constant, but Eqn. (3.21) only predicts this type of behavior over a very narrow field range for $E > 3 \times 10^5$ V/cm.[57] As pointed out by Gartstein and Conwell,[58] though, the PF behavior can be obtained over a wide range of field strengths simply by using a spatially correlated potential for the charge carriers. Several suggestions have been put forward as a cause for this type of correlations, of which the most notable are charge-dipole interactions[59,60] and thermal fluctuations in molecular geometries.[61] However, (ii) as recently pointed out by Pasveer *et al.*,[62] inclusion of the charge carrier density, ρ, into the GDM will also govern a Poole-Frenkel like behavior over a wide region of field strengths.[e] These authors also demonstrated that the ρ dependence of μ is, in general, more

---

[d]The Gaussian shape of the DOS is suggested by the Gaussian profile of the (excitonic) band and by the recognition that the polarization energy is determined by a large number of internal coordinates each varying randomly by small amounts.[26]

[e]The observations by Pasveer *et al.* was based on a master equation approach and has been reproduced by Jakobsson using Monte Carlo simulations.[63]

important than the field dependence, but that a field dependence is still required to describe the mobility, i.e., $\mu(\rho, E, T)$, at low temperatures and high fields. (iii) Finally, it is known that $\ln(\mu)$ is, for some systems, better described as a linear function of $1/T$, than as a linear function of $1/T^2$. Since this behavior, i.e., the $1/T$ dependence, is retained if the Miller-Abrahams formulas is replaced by jumping rates derived from Marcus theory, the $1/T$ dependency was originally interpreted as a fingerprint of polaron formation.[f] Although the fingerprint issue is still a matter of some controversy,[65] it is generally recognized that polaron formation should be accounted for in materials with a strong electron-phonon coupling.

For further discussions on hopping theory, we refer the reader to the excellent reviews of Walker *et al.*[66], Coehoorn *et al*[67], and Arkhipov *et al.*[68]

3.6 Charge transport in well-ordered systems

When it comes to charge transport in well-ordered organic materials, the archetypal systems are the organic molecular crystals which display very limited energetic and spatial disorder. In discussions on the impact of the electron-phonon (e-ph) coupling in these systems the distinction is, in general, not made between systems with weak or strong e-ph coupling (although the taxonomy in Fig. 2.3 might give this impression), but rather on account of whether or not it is the local or the nonlocal e-ph coupling that dominates the transport characteristics. While the former refers to the modulation of the onsite energies by both intramolecular (internal) and intermolecular (external) vibrational degrees of freedom and is the key interaction present in the Holstein molecular crystal model (MCM),[52,69] the later concerns the modulation of the transfer integrals by lattice phonons which constitutes the major interaction in Peierls models[70] such as the Su-Schrieffer-Heeger (SSH) Hamiltonian.[71,72] In general, the transport characteristics will depend on the influence of both the local and the nonlocal electron-phonon interactions.

The Hamiltonian including (explicitly) the electron-phonon (e-ph) interaction is obtained from Eqn. (3.9) by expanding E_m and V_{mn} in a power (or Taylor) series of the phonon coordinates.[73] In the linear e-ph coupling approximation, the Holstein model for a molecular crystal with only one excess electron is obtained when nonlocal e-ph terms are omitted. The Holstein model Hamiltonian then reads:

$$H = -t_m \sum_{i,j} c_i^\dagger c_j - g \sum_i c_i^\dagger c^i (a_i + a_i^\dagger) + \omega_0 \sum_i a_i^\dagger a_i, \qquad (3.22)$$

where c_i ($c_i^\dagger$) and a_i ($a_i^\dagger$) are, respectively, annihilation (creation) operators for fermions and intramolecular phonons of frequency ω_0 on site i,[g] t_m is the electron inter-site resonance integral, and g is a local electron-phonon (e-ph) coupling constant.

---

[f]It should be pointed out that it is possible to deduce the Miller-Abrahams jump rate equations from Marcus theory in the classical limit under the assumption that $0 < \Delta E \ll E_\lambda$.[64]

[g]Note that the molecules in the Holstein model are diatomic units with phonons that corresponds to local vibrations of the internuclear separation distance.

Within this model, the setting in of a polaronic regime is directly related to the magnitude of two parameters which are often introduced in this field: $\lambda \equiv g^2/(2t_m\omega_0)$, which measures the energetic convenience to form a bound state, and $\alpha \equiv g/\omega_0$, which controls the number of excited phonons to which the charge couple. For polarons to form, both conditions $\lambda > 1$ and $\alpha > 1$ have to be satisfied, corresponding to (i) a lattice deformation energy gain, $E_p = -g^2/\omega_0$, larger than the loss of bare kinetic energy (of the order of half the bandwidth,[h] $\sim -2t_m$) and (ii) a strong reduction of the effective hopping matrix element due to a sizeable local displacement of the nuclear positions. However, from the definitions of λ and α one can immediately recognize that since $\lambda = (\alpha^2/2) \cdot (\omega_0/t_m)$, a crucial role is played by the adiabatic ratio ω_0/t_m. In essence, this ratio tells us weather it is the electrons ($\omega_0 \ll t_m$) or the phonons ($\omega_0 \gg t_m$) that constitutes the faster subsystem of the two. When $\omega_0 \ll t_m$ the electrons very rapidly readjust their motions to match the motion of the much slower nuclei and the adiabatic approximation[i] may be used to describe the self-trapped states. In this case the condition for a large λ is more difficult to realize than $\alpha > 1$ and polaron formation will therefore be determined by the more restrictive $\lambda > 1$ condition. The opposite is true when the system is in the nonadiabatic regime, i.e., when $\omega_0 \gg t_m$.

A significant insight into polaron transport has been obtained from the analytical results derived by Holstein in his seminal work.[52,69] In particular, the theory predicts the temperature dependence of mobility with respect to the strength of the local electron-phonon (e-ph) coupling constant. In the case of weak local e-ph couplings ($g^2 \ll 1$), the mobility is dominated by tunneling and display a bandlike temperature dependence ($\mu \sim T^{-n}$, where $n > 0$) in the full range of temperatures.[79] For intermediate couplings ($g^2 \leq 1$), the mobility is bandlike at low temperatures but will, due to a significant increase in hopping contribution, exhibit a weaker temperature dependence at high temperatures. For strong local couplings ($g^2 \gg 1$), three distinct temperature regimes occur: (i) at low temperatures the mobility is bandlike, (ii) as the temperature increases, the hopping term starts to dominate, and the mobility exhibits a crossover from coherent transport to incoherent temperature-activated transport, and (iii) if the system can reach very high temperatures at which the thermal energy becomes large enough to dissociate the polaron, the residual electron is scattered by thermal phonons and as a result the mobility decreases again with temperature.

Despite its qualitative agreement with experiments, transport theories based solely on the original Holstein molecular model cannot fully describe the charge-transport mechanisms in organic materials. In particular, the diatomic treatment of the molecular sites in the Holstein model fails to capture the complex dynamics of the multiatomic configurations of real molecules. One way to handle this

---

[h] This value can be obtain, in the most simple approach, from the "energy splitting in dimer" (ESD) method,[74,75,76,77] which is based on the realization that at the transition point of a symmetric dimer, where the charge is equally delocalized over both points, the energy difference $E_2 - E_1$ between the adiabatic states Φ_1 and Φ_2 will correspond to $2t_{12}$. A further simplification is to apply Koopmans' theorem (KT),[78] such that, e.g., $t = (\epsilon_{\text{LUMO}+1} - \epsilon_{\text{LUMO}})/2$.

[i]Also known as the Born-Oppenheimer approximation it involves the complete neglect of the nonadiabaticity operator in Eqn. (3.10) and is often rationalized on account of the significantly higher velocities of the much heavier nuclei.

problem is presented in Paper IV where we employ the Su-Schrieffer-Heeger (SSH) Hamiltonian at the atomistic level and study the impact of the electron-lattice dynamics on the transport properties in a model molecular crystal system. In this work time-independent inter-molecular transfer integrals was used, which means that only local e-ph coupling was considered. Troisi and Orlandi, however, recently showed that variations in transfer integrals due to thermal fluctuations of the lattice can be of the same order of magnitude as the corresponding average values.[80] This is a clear indication that also the nonlocal intermolecular electron-phonon coupling must be considered.[j] Following up on these results, Troisi and Orlandi developed a one-dimensional semiclassical frontier orbital model[k] to compute the (temperature dependent) charge carrier mobility in the presence of thermal fluctuations of the electronic Hamiltonian.[84] In particular, this model accounts for non-local coupling with molecular motions restricted to lateral displacements only and exclude modulations of ϵ_i and t_i due to intramolecular vibrations. It is found from numerical simulations that this type of dynamics will induce strong localization of the charge carrier at room temperature without reference to polaron formation, which could explain contrasting experimental observations pointing sometimes to a delocalized "bandlike" transport[35,85] and sometimes to the existence of strongly localized charge carriers.[86]

It should be noted that several attempts have been made to extend the microscopic transport theory for the case where both local and nonlocal couplings are operative, most notably by Silbey and co-workers,[87,88,89] Bobbert and co-workers,[90,91] and Kenkre *et al.*[92]. Neither of these is, however, without flaws. Both the Bobbert approach and the Silbey approach build on extensions of the Holstein theory, but omits specific terms which, although the theories yields qualitative results in agreement with experiment, raises questions about the validity of the range of both models. Also the approach adapted by Kenkre *et al.* is based on the Holstein model, but generalized to higher dimensions. It was found to reproduce the temperature dependence and anisotropy of charge transport in naphtalene very well, but the values of the electronic coupling required for the fitting are significantly smaller than estimates obtained from, e.g., DFT and INDO calculations.

As a final remark, it is important to stress that only in truly ultrapure single crystals is it reasonable to assume that the energetic disorder of real systems can be considered small. In general, chemical impurities within the crystals will introduce localized states that serve to trap charge carriers who then require thermal activation to be released. Transport at low temperatures is therefore dominated by a mechanism where thermal activations transfer the carrier from the distribution of trapping centers to the transport band, where they diffuse for a while until they are trapped again. This behavior, accounted for in the multiple trapping and releasing (MTR) model,[93] is unlike hopping wherein transport takes place between the localized sites themselves.

---

[j]Note that experimental evidence to support a strong dependence of the transfer integrals on intermolecular motion has been found in many organic dimers.[81,82,83]

[k]With individual molecules as transport sites and one molecular orbital per molecule.

Methodological approach

The research presented in Papers I-V included in this thesis is intimately related to electron-lattice dynamics in the π-conjugated systems. For these studies we use a methodological approach originally proposed by Block and Streitwolf[94] with a model Hamiltonian extended to three-dimensional systems by Åsa Johansson[95] and myself[96,97] in collaborations with our supervisor Prof. Sven Stafström. The general considerations addressed within this methodology are presented in Sec. 4.1, followed by a detailed account in Sec. 4.2 of the model Hamiltonian used to describe the molecular systems of interest. In Secs. 4.3 and 4.4 we then derive the relationships used to obtain information about the static properties and dynamical behavior of these systems on the form in which they are treated within the program used to extract this data numerically.

4.1 General considerations

In our approach, we obtain the time-dependence of the electronic degrees of freedom from the solutions to the time-dependent Schrödinger equation,

$$i\hbar|\dot{\Psi}\rangle = \hat{H}_{\mathrm{el}}|\Psi\rangle, \tag{4.1}$$

with $|\Psi(t)\rangle \equiv |\Psi\rangle$, and determine the ionic motion in the evolving charge density distribution by simultaneously solving the lattice equation of motion within the potential field:

$$M_i\ddot{\mathbf{r}}_i = -\nabla_{\mathbf{r}_i}\langle\Psi|\hat{H}|\Psi\rangle. \tag{4.2}$$

Here, $\hat{H}$ ($\hat{H}_{\mathrm{el}}$) is the (electronic) Hamiltonian and $\mathbf{r}_i$ and M_i the position and mass of the i th atom, respectively. This type of calculations can be computationally very demanding and hence require approximate treatments of both $\hat{H}$ and $|\Psi\rangle$.

4.2   Model approximations

The materials of relevance for this thesis are all π-conjugated hydrocarbon systems for which the energy gap between the σ bonding and anti-bonding states is large compared to the phonon and polaron energies and of the order of those energies involved in covalent bond breaking. For our purposes it is hence sufficient to treat the σ-electrons as fully localized to the bonds which they are involved in and the wave function for the molecular states as separable with the same σ-electron wave function for all molecular states (the π-electron approximation).[98] The total electronic energy of the system can then be written as

$$E = \langle \Psi | \hat{H} | \Psi \rangle = \langle \Psi_\sigma | \hat{H}_\sigma | \Psi_\sigma \rangle + \langle \Psi_\pi | \hat{H}_\pi | \Psi_\pi \rangle = E_\sigma + \langle \Psi_\pi | \hat{H}_\pi | \Psi_\pi \rangle, \qquad (4.3)$$

where H_σ and H_π refer to the Hamiltonian of the σ- and π-electron subsystems, respectively. Since E_σ is assumed to be simply a constant, the relationship $E_\pi = \langle \Psi_\pi | \hat{H}_\pi | \Psi_\pi \rangle$ can be used to find the optimum π-electron MOs, which we expand in a linear combination of atomic orbitals (the LCAO MO approximation) using a minimal basis set of only one $2p_z$ orbital per site. The π-electron model Hamiltonian is derived below from the independent electron tight-binding model introduced in Secs. 3.1 and 3.2 and relies on an approximation scheme introduced by Su, Schrieffer and Heeger (SSH) for studies of the electron-lattice dynamics of quasi-one-dimensional systems, but is here extended to encompass also three-dimensional structures. A single unique parameter set is then used for obtaining all properties of a given system.

   The essential elements in implementing this model are the choice of the functional forms for the different energy contributions to the system. In the general case of three-dimensional molecules (schematically depicted in Fig. 4.2) a standard classic force field potential such as CHARMM (Chemistry at HARvard Macromolecular Mechanics)[99] can be used to calculate the energy contribution from the σ-bonds. Neglecting the contributions from both Coulomb and van der Waals interactions on account of the small corrections to the overall energy that these contributions are expected to have on the systems, the force field potential then read:

$$E_\sigma = \frac{K_1}{2} \sum_{\langle ij \rangle} (r_{ij} - a)^2 + \frac{K_2}{2} \sum_{\langle ijk \rangle} (\vartheta_{ijk} - \vartheta_0)^2 + K_3 \sum_{\langle ijkl \rangle} (1 - \cos(\theta_{ijkl} - \theta_0)). \; (4.4)$$

Here, K_1, K_2, and K_3 are force field constants for the stretching, bending, and twisting of bond lengths, r_{ij}, bond angles, ϑ_{ijk}, and dihedral angles, θ_{ijkl}, around the undimerized state $(a, \vartheta_0, \theta_0)$, and the angle bracketed summation indices are used to emphasize that only nearest neighbors are considered. The total cost in energy, E_{tot}, due to lattice distortions is then obtained by supplementing Eqn. (4.4) with the contribution from the kinetic energy of the ions, i.e.,

$$E_{\text{tot}} = E_\sigma + \frac{1}{2} \sum_{n=1}^{N} M_n \dot{\mathbf{r}}_n. \qquad (4.5)$$
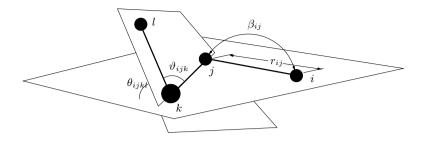
Figure 4.1. Illustration of all variables that enter the Hamiltonian of the system.

For the π-electron subsystem it is necessary to adopt a quantum mechanical description of the system in order to be able to capture the fundamental physics of, e.g., phonon excitations and polaron formation, both of which requires energies comparable to the gap between π bonding and anti-bonding states. Treating the resonance integrals, β_{ij}, in the Mulliken approximation,[100] i.e., as proportional to the overlap integrals, S_{ij}, by a constant k, the energy contribution from the π-electron system then read

$$\hat{H}_\pi = -k\sum_{\langle ij \rangle} S_{ij}[\hat{c}_j^\dagger \hat{c}_i + \hat{c}_i^\dagger \hat{c}_j], \qquad (4.6)$$

where $\hat{c}_i^\dagger$ ($\hat{c}_i$) creates (annihilates) an electron on site i and, assuming a tight-binding approach, the summation run over nearest neighbors only. Analytical formulas for S_{ij} between $2p$ Slater type atomic orbitals $\mathbf{p}_{\pi,i}$ and $\mathbf{p}_{\pi,j}$ on sites i and j (arbitrary directions) have been obtained by Hansson and Stafström[101] from the master formulas of Mulliken *et al.*[102] Expanded to first order around the undimerized state, it is easy to show that for systems where all $2p$ Slater type atomic orbitals are orthogonal to the bond plane

$$S_{ij} = k^{-1}\cos(\Phi_{ij})[t_0 - \alpha(r_{ij} - a)], \qquad (4.7)$$

where $\Phi_{ij} = \arccos(\mathbf{p}_{\pi,i} \cdot \mathbf{p}_{\pi,j}/|\mathbf{p}_{\pi,i}||\mathbf{p}_{\pi,j}|)$ is the angle between $\mathbf{p}_{\pi,j}$ and the projection of $\mathbf{p}_{\pi,i}$ along the interatomic bond axis, and

$$t_0 = A \cdot (15 + 15a\zeta + 6(a\zeta)^2 + (a\zeta)^3), \qquad (4.8)$$
$$\alpha = A \cdot a\zeta^2(3 + 3a\zeta + (a\zeta)^2), \qquad (4.9)$$

with $A = k \cdot (e^{-a\zeta}/15)$ and $\zeta = 3.07$ Å^{-1} for the $2p$ orbitals of carbon,[101] are parameters referred to as the bare hopping integral and the electron-phonon coupling constant, respectively. Equations (4.6)–(4.9) are the relevant formulas for the π-electrons in the systems treated in this thesis. Note though that if the orthogonality condition is not satisfied by all $\mathbf{p}_\pi$ vectors, π-electrons will mix with the σ-bonding system which would hence require an exact treatment also of this part of the Hamiltonian.

4.3 Statics

Having defined our model Hamiltonian, $\hat{H}$, the next step is to determine the parameter set that most accurately reproduce such properties of the real system as, e.g., the atomic configuration, the distribution of charge, and the band gap energy. This is a multi-objective optimization problem that can be solved efficiently using evolutionary algorithms (EA).[103] An EA is a generic population-based meta-heuristic optimization algorithm inspired by the mechanisms of "natural selection" where candidate solutions to the optimization problem play the role of individuals in a population, and a fitness function is designed to rank the optimality of a solution against all other candidate solutions. Evolution of the population then takes place after the repeated application of operations designed to mimic reproduction, mutation, recombination, and selection.

An ideal fitness function correlates closely with the algorithms goal, and yet may be computed quickly.[103] For the problem at hand the first of these criteria implies that the fitness function should be stated in terms of the accuracy by which molecular properties obtained from *ab initio* calculations or experimental observations are reproduced by the candidate solution. The second criteria concerns the efficiency by which each candidate solution can be retrieved and evaluated. In this case it is the first of these two steps that is time consuming since the properties of the system need to be evaluated at the variational minimum of the total energy with respect to the atomic configuration. These calculations are carried out self-consistently for each candidate (Hamiltonian) parameter set, $\mathbf{x}$, using, e.g., the resilient propagation method RPROP.[104,105] In order to keep the molecular size of the system during these procedures, we use the method of Lagrangian multipliers to include the constraint that the total change in bond lengths should amount to zero,[106] i.e., $\sum_{\langle ij \rangle}(r_{ij} - a) = 0$, which can be incorporated into the model by simply subtracting a constant term in the "distance spring part" of Eqn. (4.4) such that

$$\frac{K_1}{2}\sum_{\langle ij \rangle}(r_{ij} - a)^2 \rightarrow \frac{K_1}{2}\sum_{\langle ij \rangle}\left(r_{ij} - a - \frac{2\alpha}{K_1}\langle \rho \rangle\right)^2, \qquad (4.10)$$

where $\langle \rho \rangle$ is the mean density of charge in the system.

To shed light as to how this scheme can be carried out in practice, we take as an example the situation where the primary objective is to reproduce the *ab initio* bond lengths, r_{ij}, and band gap energies, E_g, of some particular molecule. A possible fitness function, f, for candidate solutions, $\mathbf{x}$, would then be,

$$f(\mathbf{x}) = |E_{g,\,ab} - E_{g,\,oc}(\mathbf{x})| + \sum_{\langle ij \rangle}|r_{ij,\,ab} - r_{ij,\,oc}(\mathbf{x})|, \qquad (4.11)$$

where *ab* denote values obtained from *ab initio* calculations and *oc* those obtained using the optimized configuration of the ions for each candidate parameter set. The later are, as already mentioned, retrieved from the self-consistent solutions to the following equation

$$\nabla_{\mathbf{r}_i} E_{\text{tot}} = \nabla_{\mathbf{r}_i}\langle \Psi_0|\hat{H}_\pi + \hat{H}_{\text{latt}}|\Psi_0\rangle = \nabla_{\mathbf{r}_i}[\langle \Psi_0^\pi|\hat{H}_\pi|\Psi_0^\pi\rangle + E'_{\text{latt}}] = 0 \qquad (4.12)$$

where $|\Psi_0\rangle$ is the state that minimize E_{tot} and E'_{latt} is the lattice energy as specified in Eqn. (4.5) but modified in accordance with Eqn. (4.10). The evolutionary algorithm can then be employed to find the optimal parameter set that minimizes f with respect to $\mathbf{x}$ by repeatedly modifying a population of candidate solutions $\{\mathbf{x_i}\}$ over a predefined number of generations n_g. At each step, the algorithm generates n_e children (new candidates) that are exact copies of the three individuals (present candidates) with the best fitness values, n_m children that are uniformly selected individuals with random numbers of normal distribution appended to each vector element, and n_c children that are weighted arithmetic means of two parents chosen through roulette selection within the current population. For a continuous population size of 20 individuals evolving over n_g=100 generations with n_e=3, n_m=6, and n_c=11, an optimal parameter set that minimizes f is typically found within 30 to 40 generations.

4.4 Dynamics

We are now finally at a position to outline and further develop the finer details of the methodological approach which was briefly sketched in Sec. 4.1. However, since we are interested in non-trivial dynamics we must first extend our model Hamiltonian to also include external forces that can act to perturb the otherwise static properties of the system. In this thesis, we focus mainly on field induced charge carrier dynamics, but study also excitation dynamics. As the later situation do not add to the methodological description required for the former, we only need to modify our model Hamiltonian by incorporating the impact of an externally applied electric field, $\mathbf{E}(t)$.

In our approach we take the field into account in the Coulomb gauge, i.e., by a scalar potential. Since periodic boundary conditions are not applicable in the Coulomb gauge, this will restrict us to use only finite sized systems. We further assume that the electric field is uniform in space and constant in time after a smooth turn on described by a half Gaussian function of width t_w centered at t_c. The external electric-field contribution to the Hamiltonian then reads

$$\hat{H}_E = |e| \sum_i \mathbf{r}_i \mathbf{E}(t)(\hat{c}_i^\dagger \hat{c}_i - 1), \tag{4.13}$$

where, in the direction of the electric field, $\hat{e}$,

$$\mathbf{E}(t) = \begin{cases} E_0 \exp[-(t - t_c)^2/t_w^2]\hat{e} & t < t_c, \\ E_0 \hat{e}, & \text{otherwise.} \end{cases} \tag{4.14}$$

Supplementing this contribution to H_π, we then arrive at the following expression for the electronic Hamiltonian:

$$\hat{H}_{\text{el}} = \hat{H}_\pi + \hat{H}_E = \sum_{\langle ij \rangle} \hat{c}_i^\dagger h_{ij}(t)\hat{c}_j - |e| \sum_i \mathbf{r}_i \mathbf{E}(t). \tag{4.15}$$

Note that a similar onset behavior as in Eqn. (4.14) is obtained for $E(t) = 0$ at $t < t_s$, $\frac{1}{2}E_0 \left[1 - \cos(\pi \frac{t-t_s}{t_f-t_s})\right]$ at $t_s < t < t_f$, and E_0 otherwise, but with the advantageous possibility of controlling the time period $[t_s, t_f]$ for the onset of $E(t)$.

Having defined the constituent parts of $\hat{H}$, it follows that Eqns. (4.1) and (4.2) are coupled via the one-electron density matrix elements, $\rho_{nm}(t)$, and therefore must be solved simultaneously. Within the mean-field approximation we make the ansatz[94] that $\rho_{nm}(t) = \sum_{\nu=1}^{N} C_{n\nu}^{*}(t) f_{\nu} C_{m\nu}(t)$, where $f_{\nu} \in [0,1,2]$ is the time-independent occupation number of the ν:th time-dependent molecular orbital $|\psi_{\nu}(t)\rangle$ and $C_{n\nu}(t)$ is the time-dependent expansion coefficient of a linear combination of atomic orbitals, $|\psi_{\nu}(t)\rangle = \sum_{n=1}^{N} C_{n\nu}(t)|\phi_n\rangle$. Using the generalized Hellmann-Feynman theorem for the ionic forces,[107] Eqns. (4.2) then resolves into

$$M_{n'}\ddot{\mathbf{r}}_{n'}(t) = -\sum_{n,m=1}^{N}\sum_{\nu=1}^{N} f_{\nu}C_{n\nu}^{*}(t)\,\langle\phi_n|\nabla_{\mathbf{r}_{n'}}\hat{H}(t)|\phi_m\rangle\,C_{m\nu}(t), \qquad (4.16)$$

where $C_{n\nu}(t)$ is obtained from the following equations (as derived from Eqn. (4.1)):

$$i\hbar\dot{C}_{n\nu}(t) = -e\mathbf{r}_n\mathbf{E}_0(t)C_{n\nu}(t) - \sum_{m\in\langle nm\rangle}\beta_{nm}(t)C_{m\nu}(t). \qquad (4.17)$$

The coupled differential equations (4.16) and (4.17) constitute an ordinary differential equation initial value problem (ODE IVP) and are solved numerically using a Runge-Kutta method (in the rksuite_90 package[108,109]) of order 8 with step-size control, which in practice means a time step of about 10 as. Furthermore, we use a "global time step" of 1 fs and take as the starting wave function the solution to the time-independent Schrödinger equation of the atomic configuration at $t = 0$, the later of which is obtained from a complete relaxation of atomic positions.

One of the greatest advantages with this method is that it enables studies of both nonadiabatic and adiabatic dynamics and the intrinsic and extrinsic properties that govern transitions between the two. For this reason it becomes necessary to probe the adiabaticity of the system during simulations. In order to do so, we first express the normalized time-dependent MOs, $|\psi_p(t)\rangle$, in a basis of instantaneous eigenfunctions, $|\phi_q\rangle$. Expanding $|\phi_q\rangle$ in the same basis set as $|\psi_p(t)\rangle$,

$$|\varphi_q\rangle = \sum_{n''=1}^{N} B_{n''q}|\phi_{n''}\rangle, \qquad (4.18)$$

with expansion coefficients $B_{n''q}$ derived from the time-independent Schrödinger equation $-\sum_{j=1}^{N}\beta_{ij}(t)B_{jq} = \epsilon_q B_{iq}$, we obtain, at each time step t during simulations, a relationship between the two sets of expansion coefficients of the form $C_{n'p}(t) = \sum_{q=1}^{N} B_{n'q}\alpha_{qp}(t)$, where the elements $\alpha_{qp}(t) = \langle\varphi_q|\psi_p(t)\rangle$ are used to define the time-dependent occupation number of the instantaneous eigenstates as

$$n_{\nu}(t) = \sum_{\mu=1}^{N} f_{\mu}|\alpha_{\nu\mu}(t)|^2. \qquad (4.19)$$

In adiabatic dynamics the occupation numbers are held fixed at their initial values, i.e., $\alpha_{\nu\mu}(t) \simeq \delta_{\nu\mu}$, and the dynamics is determined by the instantaneous eigenfunctions $|\varphi_\mu\rangle$. However, by simultaneously solving Eqns. (4.16) and (4.17) we allow for non-adiabatic transitions to occur which are implied in the $n_{\nu}(t)$-spectrum by multiple state occupancy and rapid interstate transitions.
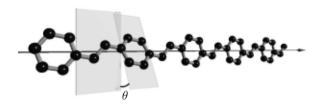
Comments on papers

Having detailed the theoretical framework of which I have been a part of developing, the purpose with this chapter is to give a brief introduction to the papers included in this thesis and highlight the main results that were obtained. In Sec. 5.1 is presented the results of Papers I-III dealing with properties of intrachain transport in conjugated polymers (CPs) using poly(*para*-phenylene vinylene) as a model system. The results presented in Sec. 5.2 for Papers IV-V concern, respectively, the transport and relaxation dynamics in molecular crystals (MCs) using the pentacene single crystal as a model system. In this context I would like to point out that although I have performed all calculations and written most of the text in Papers I-II and IV-V, I have been firmly advised by my supervisor and coauthor Prof. Sven Stafström. It should also be mentioned that Paper III is a collaboration between myself, Prof. Sven Stafström and PhD Mathieu Linares, where my contribution mainly concerned program modifications for data acquisition from the TINKER software package used for the study (the methodology of which is presented below) as well as participation in the analysis of the system dynamics.

5.1 Electron-lattice dynamics in CPs

Organic conjugated polymers have, as previously noted, emerged as a highly promising class of materials for electronic, photovoltaic, and optoelectronic applications. Considerable experimental and theoretical efforts have therefore been devoted to understand the basic properties of these systems. Among the most vividly studied conjugated polymers is poly(*para*-phenylene vinylene) (PPV), a molecule with a repeat unit consisting of a phenylene ring and a vinylene segment, the ball-and-stick model of which is presented in Fig. 5.1. Although surpassed by other materials for use in real devices, it is still considered to be an excellent

Figure 5.1. A poly(*para*-phenylene vinylene) (PPV) chain of five monomers with phenylene ring torsions. The torsion angle, θ, between the bond planes of the first vinylene group and the second phenylene ring is highlighted.

prototypical system for π-conjugated polymers.

The ground state of the isolated PPV molecule is that of a planar chain, but the potential energy required to induce the type of small non-zero torsion angles, θ, between the phenylene ring and the vinylene segment (see Fig. 5.1) is exceedingly small. For instance, the energy difference between a planar PPV chain and a PPV chain with phenylene ring torsion angles θ of $\sim 7°$ is less than 1 meV.[110] This is also evident from x-ray diffraction studies of the crystalline phase of PPV, where the experimental results suggests a nonplanar thermal-averaged chain conformation with thermally driven large-amplitude phenylene ring liberation. Since phenylene ring torsion will reduce the interatomic interaction between vinylene segments and phenylene rings along the molecular backbone, this would explain, e.g., the thermochromic blue-shift observed in the spectrum of the PPV derivative MEH-PPV.[111] It is also believed that ring torsion will influence the transport characteristics of the material, in particular the intrachain transport processes, although the details concerning the physics of these processes are not yet fully understood. The studies in Papers I-II, briefly presented below, intend to bridge at least a part of this gap.

5.1.1 Paper I: Transport along chains with static ring torsion

In paper I we focus on the impact of ring torsion due to steric effects and torsional modes with very low frequencies.[112,113] A static picture was therefore adopted for the phenylene ring torsion angles of the system (henceforth denoted as $\{\theta_n\}$) and its impact on the transport of charge carriers along the molecular backbone studied. In the limit of zero applied field any finite fluctuations in the phenylene ring torsion angles will lead to a localization of the charge and a nonadiabatic transport process. When an external electric field is applied across the chain the barriers for charge transport imposed by the torsion of the phenylene rings will be reduced and a crossover to adiabatic drift transport is possible. This crossover occurs at higher and higher electric field strengths for increasing magnitudes of the variations in $\{\theta_n\}$. The sensitivity for such transitions in the case of random variations in $\{\theta_n\}$ is strong and in systems with $\theta_n \in [0°, 20°]$ adiabatic transport is absent already at a field strength of 5.0×10^4 V/cm.

Also presented in this paper are results from simulations performed for step-like changes in the value(s) of θ_n along the chain for which quantitative details concerning the transition from adiabatic to nonadiabatic transport are obtained. It is clear from these simulations that the strength of the barrier depends on an interdependence between the magnitude of the torsion angles associated with individual phenylene rings and the extension of the region with larger torsion angles. For small torsion angles and short barrier extensions, we find that it is the sum of the decrease in the resonance integrals of the individual rings that produces the strength of the total barrier.

5.1.2 Paper II: Transport along chains with dynamic ring torsion

In Paper II we study out-of-plane torsional modes with frequencies high enough to actually have a direct influence on the charge transport processes along the chain.[114] A mixed quantum mechanical / molecular dynamics (QMMD) simulation in the NVT ensemble at $T = 300$ K with the TINKER software package[a] (URL http://dasher.wustl.edu/tinker/) reveals that these are the dominant torsional modes at room temperature and that the time period for these modes is roughly 1.4 picosecond. The modulations of the resonance integrals at the C-C phenylene-vinylene bonds due to dynamic ring torsion therefore only imposes temporary restrictions of localization for propagating charge carriers. Incorporating this type of dynamics into our model, we focus in this paper on the impact of dynamic phenylene ring torsion on the intrachain transport processes. Our previous results from Paper I then provide information only about the instantaneous picture in this type of systems with the most important result being the detailed analysis of the barrier crossing which still applies.

Simulations were performed on both unbiased and biased systems. In particular, we find that charge carriers in the unbiased system move as a consequence of the continuous changes made to the potential energy surface by the dynamics of ring torsion. Furthermore, we also observe nonadiabatic interstate transitions when the charge carrier is either destabilized by the torsion of rings within the region where it resides or when it breaches a potential energy barrier as a result of the time evolution of the torsion angles that constitutes the barrier. In the case of the biased systems, we find that the dynamics of ring torsions can lead to a nonadiabatic transport process. In Fig. 5.2, where the results from a simulation on a system across which an external electric field is turned on smoothly over a time interval of $t \in [1400, 1600]$ femtoseconds, such an occasion can be observed at $t \simeq 1900$ femtoseconds. During a small time frame, we then observe a reallocation of charge density from one end of the system to the other (left panel). This process involves, with reference to the time evolution of the occupation number of occupied levels displayed in the center panel, a transition from the localized polaron level to a delocalized level followed by stabilization of this delocalized level into a new polaronic state. From the time evolution of the strength of the resonance integrals, $\{\beta_n(\theta_n)\}$, across each interconnecting bond between a phenylene ring and

---

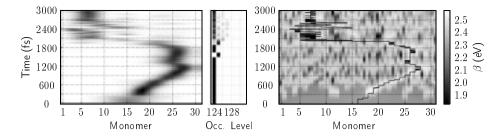[a]A methodological approach which is further detailed in Sec. 5.1.3.

Figure 5.2. The time evolution of the density of charge (left panel), the occupation number per occupation level (center panel), and the resonance integral strength for each interconnecting bond between a phenylene ring and a vinylene group (right panel) is displayed. These results are obtained from a simulation on a PPV chain with 31 phenylene rings across which an external electric field is raised from $E_0 = 0$ V/cm to 5.0×10^4 V/cm^2 during a time period of 200 femtoseconds (fs), initiated at $t = 1400$ fs. Note that the solid line in the right panel is used to highlight the position of the center of the local density of charge (left panels).

a vinylene segment, as displayed in the right panel of Fig. 5.2, it is evident that this process is brought about by the torsional motion of the phenylene rings. We hence conclude that intrachain transport processes at room temperature involves both nonadiabatic effects and the dynamics of the polaron state.

5.1.3 Paper III: Localization due to ring torsion dynamics

To gain further insight into the impact of ring torsion dynamics on the electronic properties in PPV we employed the previously mentioned combined quantum mechanical / molecular dynamics (QMMD) approach, which enables us to include temperature in an explicit fashion.

In brief, we performed molecular dynamics simulations on PPV oligomers using the TINKER molecular software package (URL http://dasher.wustl.edu/tinker/). For the Hamiltonian we used a MM3 force field[115,116,117] for the nuclear motion combined with the quantum mechanical Pariser–Parr–Pople (PPP) model[40,118,119] for the π-electron system.[b] Compared to the SSH Hamiltonian used in the previous studies, the PPP model includes also the one- and two-center electron-electron repulsion integrals. Similar to the approach detailed in Sec. 4.2, the effect of torsion (around a given π bond) on the bond conjugation is included in the model by imposing a modulation of the resonance integral of the form:

$$\beta_{ij} = \cos(\theta_{ij})\beta_{ij}^{(p)}, \tag{5.1}$$

where $\beta_{ij}^{(p)}$ is the resonance integral for the planar conformation. The MD simu-

---

[b]Compared to harmonic force field potentials such as CHARMM,[99] Allinger's MM3 method uses, in particular, a quartic Taylor series expansion to approximate the Morse potential for bond stretch and a sextic expansion for angle bend.

lations were performed in the NVT canonical ensemble[c] using periodic boundary conditions with a very large super cell ($20 \times 20 \times 20$ nm) to simulate an isolated chain in vacuum. The full time period of the simulation is 20 picoseconds with a time step of 1 atosecond. Every femtosecond during the simulation we extract the LCAO expansion coefficients for the molecular orbitals (MOs) of the PPV oligomer and, being primarily interested in the electron localization properties of the system, calculate the inverse participation ratio (IPR). The IPR for the j:th MO is defined as:

$$IPR_j = \frac{\sum_{i=1}^{N} C_{ij}^4}{\left(\sum_{i=1}^{N} C_{ij}^2\right)^2},$$ (5.2)
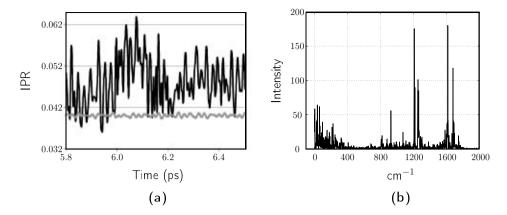
where C_{ij} is the LCAO expansion coefficient at site i and N the number of sites (carbon atoms) in the system. For an infinite system with an orthonormal basis, the value of IPR_j would vary from zero for extremely localized states to one for fully delocalized states.

The thermally induced dynamics of the PPV oligomer involves bond stretching, bond angle bending, and torsional degrees of freedom and we focus on how these geometrical changes couple to the electronic structure of the system, in particular to electron localization as described by the IPR value. Due to computational costs we limit our study to a chain of five monomer units.[d] In Fig. 5.3(a) is shown the IPR as a function of time for the highest occupied molecular orbital (HOMO) at $T = 1$ K (solid gray line) and 300 K (solid black line), respectively, during a time period of 700 femtoseconds. At $T = 1$ K all phonon mode amplitudes are small which means that the oligomer is at all times close to its planar ground state confirmation. This favors delocalization of the wave function, but since the structure of PPV is such that the HOMO has different expansion coefficients for the AOs at different sites, the value of the IPR is higher than what might be expected for the fully delocalized state in the five monomer oligomer, which would be $1/40 = 0.025$. At $T = 300$ K we see a clear effect on the localization properties due to thermally induced phonon modes. Note though that the relatively small change in the IPR value indicates that the degree of localization is rather small, which is to be expected in a system of this moderate size.

An interesting feature of the time evolution of the *IPR* for the HOMO level at $T = 300$ K are the high and low frequency oscillations that occurs with similar amplitudes. From the Fourier transform of the IPR_{HOMO} at $T = 300$ K, taken over the full simulation period, i.e., 20 ps, and displayed in Fig. 5.3(b), these components are clearly resolved. We observe low frequency components in the frequency range 0-250 cm^{-1}, as well as three other contributions around 900, 1270 and 1600 cm^{-1}. These regimes could be correlated to changes in the resonance integral strength of specific types of covalent bonds along the molecular backbone.

---

[c]A statistical ensemble representing a probability distribution of microscopic states of the system where the number of particles (N), the volume (V), of each system in the ensemble are the same, and the ensemble has a well defined temperature (T).

[d]Note that simulations over a couple of picoseconds with a chain of ten monomer units showed that the wave function is significantly localized only over 3 monomer units, which implies that the five monomer system is sufficiently large for our analysis of the influence of system dynamics.

Figure 5.3. In (a) is shown the IPR of the HOMO as a function of time at two temperatures: $T = 1$ K (solid gray) and $T = 300$ K (solid black). In (b) is shown the Fourier transform of the later (but taken during the full time period of the simulation, i.e., 20 ps).
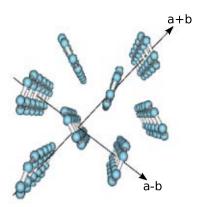
The most important changes, corresponding to the signatures in the low frequency regime and around 1270 cm^{-1}, could be traced to the dynamics of the C-C single and double bonds on the vinylene segments. The additional contributions to the IPR spectrum at 900 cm^{-1} and 1600 cm^{-1} are due to modes localized to the phenylene rings.

The C-C bond stretching of the double bond in the vinylene unit is of secondary interest in relation to the intrachain transport properties. First, the increase in IPR is rather limited and remains essentially unchanged if we go to more extended oligomers. Second, the time scale for the associated changes in β and IPR is faster or of the same order as the time scale of polaron transport and it will therefore not reduce the polaron drift velocity to any larger extent. We therefore conclude that the single most important intrachain lattice mode which limits polaron transport along a PPV chain is the torsion of phenylene rings with respect to the vinylene segments. These results are in favor of our previously adapted approach in Papers I and II.

5.2 Electron-lattice dynamics in MCs

Organic molecular crystals (MCs) are often employed by experimentalists to obtain basic physical insight into the intrinsic properties and processes of organic molecular solids. Of these, the ultrapure single crystals, in which the crystal lattice of the entire sample is envisioned as continuous and unbroken, offers a minimal influence of extrinsically induced diagonal and off-diagonal disorder. Most vividly studied are the oligoacene single crystals and in particular the pentacene (C$_{22}$H$_{14}$) single crystal in which a hole mobility exceeding that in amorphous silicon has been measured.[120]

The fundamental limit for charge transport in these systems depends on the

Figure 5.4. The *ab*-plane of the triclinic crystal structure of pentacene, where the strongest pathways for charge transport has been highlighted.

molecular packing within the organic crystal. In the case of the (small) oligoacene molecules, the structure of the crystal is triclinic with two planar molecules in the unit cell, situated on independent centers of symmetry.[121] The intermolecular overlap in the direction of the long molecular axis is weak, and transport is thus facilitated predominantly in two dimensional molecular sheets, as depicted in Fig. 5.4 in the case of the pentacene crystal.

We have conducted two studies with respect to molecular crystals, one related to their associated transport properties (Paper IV) and the other to nonradiative relaxation dynamics (Paper V). In both of these studies we use as a model system for molecular crystals linear segments of pentacene molecules extracted from the single crystal configuration along the $a + b$ crystallographic direction (as defined in Fig. 5.4).

5.2.1 Paper IV: Transport dynamics in MCs with local e-ph coupling

In this work we study the charge carrier transport process in molecular crystals as a function of intermolecular interaction strength, J,[e] with an emphasis on the transition from adiabatic polaron drift to nonadiabatic hopping transport. The details of this transition is determined by the relative strength of J and E_p, the later of which is the energy gained by the system from the self-localization of a single charge, i.e., the polaron formation energy.[f] In particular, we can identify three different regimes for charge carrier transport in molecular solids. On the one hand we have the systems with weak intermolecular interactions ($J \ll E_p$) for

---

[e]This quantity is obtained from the energy splitting in dimer with Koopmans' theorem (ESD-KT) method, as presented in footnote h in Sec. 3.6.

[f]It was shown by Capone *et al.*[122] that λ, i.e., the energetic convenience to form a bound state, need to be larger than one for the settling in of a polaronic regime. This quantity was introduced already in Sec. 3.6, and since $J \simeq -2t_m$ (t_m being the intermolecular transfer/resonance integral), it follows from the definition of λ that $\lambda = E_p/J$.

which the small polaron localized to a single molecule is stable and transport may be analyzed in terms of hopping, and on the other hand we have the systems with strong intermolecular interaction ($J \gg E_p$) for which the localized carrier state is unstable and band transport applies. For systems in the intermediate regime ($J \sim E_p$) the polaron is delocalized over several molecular units. The dynamics of this type of systems can be analyzed with our methodological approach, which is the main focus of this work.
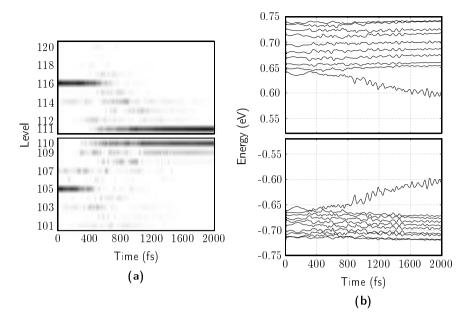
As a model system we use linear segments of pentacene molecules in the single crystal configuration [121] and introduce scaled values of the intermolecular interatomic resonance integrals of the form of Eqn. (4.7) in order to simulate different intermolecular interaction strengths, J. The time-dependence of the occupation number (see Eqn. (4.19)) is used as a measurement of the adiabaticity [123] of the system. Within our model we determine the polaron formation energy to be $E_p = 97$ meV. Covering the regime $J \in [20, 120]$ meV we then observe a shift from a nonadiabatic to an adiabatic polaron drift process. For intermolecular interaction strengths $J > 120$ meV the polaron is no longer stable and the transport becomes band like, whereas for $J \leq 20$ meV the polaron is localized to a single molecule and transport is assumed to occur through nonadiabatic hopping transport.

These observations imply that our approach can be used to study the dynamics of charge transport in the intermediate regime where neither band theory nor perturbative treatments like the Holstein model [52,69] or extended Marcus theory [56] apply.

5.2.2 Paper V: Internal conversion dynamics in MCs

In this paper we explore the dynamics of nonradiative electronic relaxation processes in molecular crystals. This is known from experiments to constitute the dominant relaxation channel from higher lying excited states in this type of systems. Typically, the process involves an ultrafast nonradiative relaxation between states of the same spin multiplicity, a process referred to as internal conversion (IC), followed by a much slower decay of the phonons induced into the system during the IC phase. Depending on the excitation energy the relaxation process can involve interstate transitions both within and between the bands of molecular crystal orbitals.

The dynamics of a typical intraband relaxation process is captured in Fig. 5.5, where the time evolution of (a) the occupation numbers and (b) the energy levels of the manifold of instantaneous eigenstates following an electron excitation across the band gap from the 105 th to the 116 th molecular crystal orbital (MCO) are displayed. These results clearly show a nonadiabatic internal conversion process towards the states closest to the band gap followed by a subsequent adiabatic decay of vibrational modes within the system accompanied by the evolution of a self-localized electron-hole species with a polaronic signature. Note that the quasistatic phase observed in the beginning of the simulation is an artifact of the way in which we introduce electron excitation into our model (as further detailed in Paper V).

Figure 5.5. The evolution of (a) the occupation numbers and (b) the energy levels of the instantaneous eigenstates as a function of time (in femtoseconds) following the excitation of an electron from the 105 th to the 116 th molecular crystal orbital in a system of ten pentacene molecules. Note that the 110 th and the 111 th levels are the highest occupied and the lowest unoccupied MCOs in the system, respectively.

When excitations are made from states well below the highest occupied MCO to states well above the lowest unoccupied MCO, the nonradiative relaxation process will also involve interband interstate transitions. Our calculations show that these events are facilitated by the transfer of energy from the electronic system to the lattice and that the phonons induced couples only to the states in the bands of MCOs to which the transition is made. It is also clear from these simulations that the relaxation process observed is limited by the interband transitions made between states of considerably different eigenenergies.

Outlook

To conclude the first part of this thesis we here provide an outlook of developmental issues that if solved would improve the applicability of the model/methodology used in the research presented in Papers I-II and IV-V. In particular:

1 The Hamiltonian introduced in Chap. 4 does not include electron-electron repulsion. To take also these interactions into account would be particularly valuable in studies of, e.g., excitons or systems with multiple charges.

2 With the currently employed classical description of the nuclei dynamics, our model is strictly speaking only valid in the high-temperature regime, i.e., where $k_B T \gg \hbar\omega_\xi$ for all phonon modes ξ. Obviously it would be beneficial to extend its applicability also towards the low-temperature regime by incorporating a quantized description of the lattice.

3 The weak interactions between molecules and their interdependence on the electron-phonon coupling dynamics is currently lacking in our model. With a full description of the intra- as well as intermolecular interactions, it would be possible to probe not only local coupling (as in Paper IV) or nonlocal coupling (as in the work by Troisi and Orlandi[80]) separately, but to actually study the full dynamics of systems with many molecules.

4 To be able to treat longer systems while keeping computational costs down, it would be beneficial to implement our method using periodic boundary conditions. This has been done by others on quasi-one-dimensional systems such as *trans*-polyacetylene[124,125,126] and generally requires that the externally applied electric field is treated as a vector potential. Within this approach,

the electronic and electric field part of the Hamiltonian can be written as

$$H_{\text{el}} = -\sum_{\langle nm \rangle} \beta_{nm}(t)[e^{i\gamma A(t)}\hat{c}_n^\dagger \hat{c}_m + \text{H.c.}], \qquad (6.1)$$

where the parameter γ is defined as $\gamma = ea/\hbar c$, with e being the absolute value of the electronic charge, a the bond length in the undimerized molecules, and c the speed of light, and $A(t)$ is a vector potential of the form $E(t) = -(1/c) \cdot (\partial A(t)/\partial t)$, introduced to describe a uniform time-dependent external electric field $E(t)$ along the chain. The modified electronic Hamiltonian Eqn. (6.1) is then incorporated into the time-dependent Schrödinger equation and the equation of motion. When solving these two coupled equations using the Runge-Kutta (RK) method previously mentioned in Sec. 4.4, we note that since the time step Δt taken by the RK solver is small compared to the characteristic time of the lattice vibration it follows that

$$A(t) = \int_{t'} \frac{\partial A(t')}{\partial t'} dt' = -c \int_{t'} E(t')dt' \simeq -c\Delta t E(t). \qquad (6.2)$$

What remains to be considered, besides the actual implementation of these relationships into the simulations software, is to evaluate exactly what type of periodic boundary condition that should be used.

It is my sincere hope that others continue to work with the model and solve these or other developmental issues, whichever they may be.

Bibliography

1. H. Shirakawa, *Autobiography, from Les Prix Nobel. The Nobel Prizes 2000*, Editor Tore Frängsmyr, [Nobel Foundation], Stockholm, 2001.

2. H. Shirakawa, *Rev. Mod. Phys.* **73**, 713 (2001).

3. T. Ito, H. Shirakawa, and S. Ikeda, *J. Polym. Sci., Polym. Phys. Ed.* **4**, 605 (1974).

4. C. K. Chiang, C. R. Fincher, Y. W. Park, A. J. Heeger, H. Shirakawa, E. J. Louis, S. C. Gau, and A. G. MacDiarmid, *Phys. Rev. Lett.* **39**, 1089 (1977).

5. H. Shirakawa, E. J. Louis, A. G. MacDiarmid, C. K. Chiang, and A. J. Heeger, *J. Chem. Soc. Chem. Commun.* **1977**, 578 (1977).

6. C. W. Tang, and S. A. VanSlyke, *Appl. Phys. Lett.* **51**, 913 (1987).

7. J. H. Burroughes, D. D. C. Bradley, A. R. Brown, R. N. Marks, K. Mackay, R. H. Friend, P. L. Burn, and A. B. Holmes, *Nature* **347**, 539 (1990).

8. A. Tsumura, H. Koezuka, and T. Ando, *Appl. Phys. Lett.* **49**, 1210 (1986).

9. J. H. Burroughes, C. A. Jones, and R. H. Friend, *Nature* **335**, 137 (1988).

10. F. Garnier, R. Hajlaoui, A. Yassar, and P. Srivastava, *Science* **265**, 1684 (1994).

11. N. S. Sariciftci, D. Braun, C. Zhang, V. I. Srdanov, A. J. Heeger, G. Stucky, and F. Wudl, *Appl. Phys. Lett.* **62**, 585 (1993).

12. G. Yu, J. Gao, J. C. Hummelen, F. Wudl, and A. J. Heeger, *Science* **270**, 1789 (1995).

13. Sony launches world's first oled tv (2007).

14. R. J. Kline, M. D. McGehee, E. N. Kadnikova, J. Liu, and J. M. J. Frechet, *Adv. Mater.* **15**, 1519 (2003).

15. M. Hamedi, R. Forchheimer, and O. Inganäs, *Nature Mater.* **6**, 357 (2007).

16. H. Sirringhaus, T. Kawase, R. H. Friend, T. Shimoda, M. Inbasekaran, W. Wu, and E. P. Woo, *Science* **290**, 2123 (2000).

17. T. Kawase, H. Sirringhaus, R. H. Friend, and T. Shimoda, *Adv. Mater.* **13**, 1601 (2001).

18. M. Berggren, D. Nilsson, and N. D. Robinson, *Nature Mater.* **6**, 3 (2007).

19. C. Reese, and Z. Bao, *J. Mater. Chem.* **16**, 329 (2006).

20. M. Born, *Z. Physik* **37**, 863 (1926).

21. M. Born, *The statistical interpretations of quantum mechanics, from Nobel Lectures, Physics 1942-1962*, Elsevier Publishing Company, Amsterdam, 1964.

22. R. S. Mulliken, *Phys. Rev.* **41**, 49 (1932).

23. R. S. Mulliken, *J. Chem. Phys.* **3**, 375 (1935).

24. A. Aviram, and M. A. Ratner, *Chem. Phys. Lett.* **29**, 277 (1974).

25. K. Sworakowski, K. Janus, S. Nešpurek, and M. Vala, *IEEE. Trans. Dielectr. Eetrl. Insul.* **13**, 1001 (2006).

26. H. Bässler, *Phys. Stat. Sol. (b)* **107**, 9 (1981).

27. A. Miller, and E. Abrahams, *Phys. Rev.* **120**, 745 (1960).

28. R. A. Marcus, *Rev. Mod. Phys.* **65**, 599 (1993).

29. D. Emin, *Phys. Rev. Lett.* **32**, 303 (1974).

30. B. Movaghar, *J. Mol. El.* **3**, 183 (1987).

31. N. F. Mott, and E. A. Davids, *Electronic processes in non-crystalline materials*, Oxford University Press, London, 1973.

32. N. F. Mott, *Electron. Power* **19**, 321 (1973).

33. W. A. Thompson, T. Penney, S. Kirkpatrick, and F. Holtzberg, *Phys. Rev. Lett.* **29**, 779 (1972).

34. A. J. Campbell, D. D. C. Bradley, and D. G. Lidzey, *J. Appl. Phys.* **82**, 6326 (1997).

35. N. Karl, *Synth. Met.* **133-134**, 649 (2003).

36. V. Coropceanu, J. Cornil, D. A. da Silva Filho, Y. Oliver, R. Silbey, and J. L. Bredas, *Chem. Rev.* **107**, 926 (2007).

37. V. Podzorov, E. Menard, A. Borissov, V. Kiryukhin, J. A. Rogers, and M. E. Gershenson, *Phys. Rev. Lett.* **93**, 086602 (2004).

38. R. Kersting, U. Lemmer, M. Deussen, H. J. Bakker, R. F. Mahrt, H. Kurz, V. I. Arkhipov, H. Bässler, and E. O. Göbel, *Phys. Rev. Lett.* **73**, 1440 (1994).

39. M. Pope, and C. E. Swenberg, *Electronic processes in organic crystals & polymers*, Oxford University Press, New York, 1999.

40. J. A. Pople, *Trans. Faraday Soc.* **49**, 1375 (1953).

41. R. A. Marcus, *J. Chem. Phys.* **24**, 966 (1956).

42. R. A. Marcus, *J. Chem. Phys.* **24**, 979 (1956).

43. R. A. Marcus, *Disc. Faraday Soc.* **29**, 21 (1960).

44. R. A. Marcus, *Ann. Rev. Phys. Chem.* **15**, 155 (1964).

45. P. W. Anderson, *Phys. Rev.* **109**, 1492 (1958).

46. N. F. Mott, *Phil. Mag.* **13**, 989 (1966).

47. N. F. Mott, *Adv. Phys.* **16**, 49 (1967).

48. H. Bässler, *Phys. Stat. Sol. (b)* **175**, 15 (1993).

49. N. F. Mott, *Phil. Mag.* **19**, 835 (1969).

50. N. F. Mott, and E. A. Davis, *Electronic Processes in Non-Crystalline Materials*, Calendron Press, Oxford, 1979.

51. N. Apsley, and H. Huges, *Phil. Mag.* **30**, 963 (1974).

52. T. Holstein, *Ann. of Phys.* **8**, 343 (1959).

53. G. C. Schatz, and M. A. Ratner, *Quantum Mechanics in Chemistry*, Dover Publication, Mineola, NY, 2002.

54. D. Emin, *Adv. Phys.* **24**, 305 (1975).

55. J. Jortner, *J. Chem. Phys.* **64**, 4860 (1976).

56. M. Bixon, and J. J, *Adv. Chem. Phys.* **106**, 35 (1999).

57. L. B. Schein, *Phil. Mag. B* **65**, 795 (1992).

58. Y. N. Gartstein, and E. M. Conwell, *Chem. Phys. Lett.* **245**, 351 (1995).

59. D. H. Dunlap, P. E. Parris, and V. M. Kenkre, *Phys. Rev. Lett.* **77**, 542 (1996).

60. S. V. Novikov, D. H. Dunlap, V. Kenkre, P. E. Parris, and A. V. Vannikov, *Phys. Rev. Lett.* **81**, 4472 (1998).

61. Y. Roichman, and N. Tessler, *Synth. Met.* **135-136**, 443 (2003).

62. W. F. Pasveer, J. Cottaar, C. Tanase, R. Coehoorn, B. P. A., P. W. M. Blom, D. M. de Leeuw, and M. A. J. Michels, *Phys. Rev. Lett.* **94**, 206601 (2005).

63. M. Jakobsson, *Monte Carlo simulations of charge transport in organic materials*, Master's thesis, Linköpings Universitet (2006).

64. Y. N. Gartstein, and E. M. Conwell, *Chem. Phys. Lett.* **217**, 41 (1994).

65. I. I. Fishchuk, A. Kadashchuk, H. Bässler, and S. Nešpůrek, *Phys. Stat. Sol. (c)* **1**, 152 (2004).

66. A. B. Walker, A. Kambili, and S. J. Martin, *J. Phys.: Condens. Matter* **14**, 9825 (2002).

67. R. Coehoorn, W. F. Pasveer, P. A. Bobbert, and M. A. J. Michels, *Phys. Rev. B* **72**, 155206 (2005).

68. V. I. Arkhipov, I. I. Fishchuk, A. Kadashchuk, and H. Bässler, *Semiconducting Polymers: Chemistry, Physics and Engineering (Vol. 1, 2^{ed})*, Wiley-VCH, Weinheim, 2006.

69. T. Holstein, *Ann. of Phys.* **8**, 325 (1959).

70. R. E. Peierls, *Quantum theory of solids*, Clarendon Press, Oxford, 1955.

71. W. P. Su, J. R. Schrieffer, and A. J. Heeger, *Phys. Rev. Lett.* **42**, 1698 (1979).

72. W. P. Su, J. R. Schrieffer, and A. J. Heeger, *Phys. Rev. B* **22**, 2099 (1980).

73. E. M. Conwell, *Phys. Rev. B* **22**, 1761 (1980).

74. M. D. Newton, *Chem. Rev.* **91**, 767 (1991).

75. K. D. Jordan, and M. N. Paddonrow, *J. Phys. C* **96**, 1188 (1992).

76. J. Cornil, J. P. Calbert, and J. L. Brédas, *J. Am. Chem. Soc.* **123**, 1250 (2001).

77. V. Lemaur, D. A. Da Silva Filho, V. Coropceanu, M. Lehmann, Y. Geerts, J. Piris, M. G. Debije, A. M. Van de Craats, K. Senthilkumar, L. D. A. Siebbeles, J. M. Warman, J. L. Brédas, and J. Cornil, *J. Am. Chem. Soc.* **126**, 3271 (2004).

78. T. Koopmans, *Physica* **1**, 104 (1934).

79. R. J. Silbey, and R. W. Munn, *J. Chem. Phys.* **72**, 2763 (1980).

80. A. Troisi, and G. Orlandi, *Phys. Rev. Lett.* **96**, 086601 (2006).

81. R. A. Binstead, J. R. Reimers, and N. S. Hush, *Chem. Phys. Lett.* **378**, 654 (2003).

82. V. Coropceanu, J. M. Andre, M. Malagoli, and B. J. L., *Theor. Chem. Acc.* **110**, 59 (2003).

83. D. Pedron, A. Speghini, V. Mulloni, and R. Bozio, *J. Chem. Phys.* **103**, 2795 (1995).

84. A. Troisi, and G. Orlandi, *J. Phys. Chem. A* **110**, 4065 (2006).

85. Y. C. Chen, R. J. Silbey, J. P. da Silva Filho, D. A. andCalbert, J. Cornil, and J. L. Brédas, *J. Chem. Phys.* **118**, 3764 (2003).

86. P. J. Brown, H. Sirringhaus, M. Harrison, M. Shkunov, and R. H. Friend, *Phys. Rev. B* **63**, 125204 (2001).

87. Y. C. Chen, and R. J. Silbey, *J. Chem. Phys.* **128**, 114713 (2008).

88. R. W. Munn, and R. J. Silbey, *J. Chem. Phys.* **83**, 1843 (1985).

89. R. W. Munn, and R. J. Silbey, *J. Chem. Phys.* **83**, 1854 (1985).

90. K. Hannewald, and P. A. Bobbert, *Appl. Phys. Lett.* **85**, 1535 (2004).

91. K. Hannewald, V. M. Stojanovic, J. M. T. Schellekens, P. A. Bobbert, G. Kresse, and J. Hafner, *Phys. Rev. B* **69**, 075211 (2004).

92. V. M. Kenkre, J. D. Andersen, D. H. Dunlap, and C. B. Duke, *Phys. Rev. Lett.* **62**, 1165 (1989).

93. P. G. Le Comber, and W. E. Spear, *Phys. Rev. Lett.* **25**, 509 (1970).

94. S. Block, and H. W. Streitwolf, *J. Phys.: Condens. Matter* **8**, 889 (1996).

95. r. Johansson, and S. Stafström, *Phys. Rev. B* **68**, 035206 (2003).

96. M. Hultell, and S. Stafström, *Chem. Phys. Lett.* **428**, 446 (2006).

97. M. Hultell, and S. Stafström, *Phys. Rev. B* **75**, 104304 (2007).

98. P. G. Lykos, and R. G. Parr, *J. Chem. Phys.* **24**, 1166 (1956).

99. B. R. Brooks, R. E. Bruccoleri, B. D. Olafson, D. J. States, S. Swaminathan, and M. Karplus, *J. Comp. Chem.* **4**, 187 (1983).

100. R. S. Mulliken, *J. Chim. Phys.* **46**, 675 (1949).

101. A. Hansson, and S. Stafström, *Phys. Rev. B* **67**, 075406 (2003).

102. R. S. Mulliken, C. A. Reike, D. Orloff, and H. Orloff, *J. Chem. Phys.* **17**, 1248 (1949).

103. R. Polio, W. B. Langton, and N. F. McPhee, *A field guide to genetic programming*, Lulu Enterprises, UK Ltd., 2008.

104. M. Riedmiller, and H. Braun, "A direct adaptive method for faster back-propagation learning: The RPROP algorithm," in *Proceedings of the IEEE International Conference on Nural Networks*, edited by H. Ruspini, 1993, pp. 586–591.

105. C. Igel, and M. Hüsken, *Neurocomputing* **50**, 105 (2003).

106. J. Fagerström, *Quantum chemical calculations of structural and electronic properties of conjugated polymers, fullerenes and some small molecules*, Ph.D. thesis, Linköpings Universitet (1996).

107. R. E. Allen, *Phys. Rev. B* **50**, 18629 (1994).

108. R. W. Brankin, and I. Gladwell, *Ann. Num. Math.* **1**, 363 (1994).

109. R. W. Brankin, and I. Gladwell, *ACM Trans. Math. Soft.* **23**, 402 (1997).

110. R. B. Capaz, and M. J. Caldas, *J. Mol. Struct.* **464**, 31 (1999).

111. K. Kong, X. L. Wu, G. S. Huang, R. K. Yuan, C. Z. Yang, P. K. Chu, and G. G. Siu, *Appl. Phys. A* **84**, 203 (2006).

112. M. N. Bussac, J. D. Picon, and Zuppiroli, *Europhys. Lett.* **66**, 392 (2004).

113. P. Prins, F. C. Grozema, and L. D. A. Siebbeles, *J. Phys. Chem. B* **110**, 14659 (2006).

114. P. Papanek, J. E. Fischer, J. L. Sauvajol, A. J. Dianoux, G. Mao, M. J. Winokur, and F. E. Karasz, *Phys. Rev. B* **50**, 15668 (1994).

115. N. L. Allinger, Y. H. Yuh, and J.-H. Lii, *J. Am. Chem. Soc.* **111**, 8551 (1989).

116. J.-H. Lii, and N. L. Allinger, *J. Am. Chem. Soc.* **111**, 8566 (1989).

117. J.-H. Lii, and N. L. Allinger, *J. Am. Chem. Soc.* **111**, 8576 (1989).

118. R. Pariser, and R. G. Parr, *J. Chem. Phys.* **21**, 466 (1953).

119. R. Pariser, and R. G. Parr, *J. Chem. Phys.* **21**, 767 (1953).

120. O. D. Jurchescu, J. Baas, and T. T. M. Palstra, *Appl. Phys. Lett.* **84**, 3061 (2004).

121. R. B. Campbell, J. Monteath Robertson, and J. Trotter, *Acta Cryst.* **14**, 705 (1961).

122. M. Capone, W. Stephan, and M. Grilli, *Phys. Rev. B* **56**, 4484 (1997).

123. H. Nakamura, *Nonadiabatic transition: Concepts, basic theories and applications*, World Scientific Publishing Co. Pte. Ltd., 2002.

124. J. F. Yu, C. Q. Wu, X. Sun., and K. Nasu, *Phys. Rev. B* **70**, 064303 (2004).

125. Z. An, C. Q. Wu, and X. Sun, *Phys. Rev. Lett.* **93**, 216407 (2004).

126. X. Liu, K. Gao, Y. Li, J. Fu, J. Wei, and S. Xie, *Synth. Met.* **157**, 380 (2007).

List of Publications

I. Magnus Hultell and Sven Stafström. Impact of ring torsion on the intra-chain mobility in conjugated polymers. *Physical Review B* **75**, 104304 (2007).

II. Magnus Hultell and Sven Stafström. Impact of ring torsion dynamics on intrachain charge transport processes in conjugated polymers. *Submitted.*

III. Mathieu Linares, Magnus Hultell and Sven Stafström. The effect of lattice dynamics on electron localization in poly-(*para*-phenylene vinylene). *Submitted.*

IV. Magnus Hultell and Sven Stafström. Polaron dynamics in highly ordered molecular crystals. *Chemical Physics Letters* **428**, 446 (2006).

V. Magnus Hultell and Sven Stafström. Nonradiative relaxation processes in molecular crystals. *Journal of Luminescence* **128**, 2019 (2008).